https://doi.org/10.5194/amt-2020-386
Preprint. Discussion started: 8 October 2020

Atmospheric Measurement Techniques Discussions

Can a regional-scale reduction of atmospheric CO_2 during the COVID-19 pandemic be detected from space? A case study for East China using satellite XCO_2 retrievals

Michael Buchwitz[1], Maximilian Reuter[1], Stefan Noël[1], Klaus Bramstedt[1], Oliver Schneising[1], Michael Hilker[1], Blanca Fuentes Andrade[1], Heinrich Bovensmann[1], John P. Burrows[1], Antonio Di Noia[2,3], Hartmut Boesch[2,3], Lianghai Wu[4], Jochen Landgraf[4], Ilse Aben[4], Christian Retscher[5], Christopher W. O'Dell[6], David Crisp[7]

[1]Institute of Environmental Physics (IUP), University of Bremen, 28334 Bremen, Germany
[2]Earth Observation Science, University of Leicester, LE1 7RH, Leicester, UK
[3]NERC National Centre for Earth Observation, LE1 7RH, Leicester, UK
[4]SRON Netherlands Institute for Space Research, 3584 CA Utrecht, The Netherlands
[5]Directorate of Earth Observation Programmes, European Space Agency (ESA), ESRIN, 00044 Frascati, Italy
[6]Cooperative Institute for Research in the Atmosphere, Colorado State University (CSU), Fort Collins, CO 80523, USA
[7]Jet Propulsion Laboratory (JPL), Pasadena, CA 91109, USA

Correspondence to: Michael Buchwitz (buchwitz@uni-bremen.de)

Abstract. The COVID-19 pandemic resulted in reduced anthropogenic carbon dioxide (CO_2) emissions during 2020 in large parts of the world. We report results from a first attempt to determine whether a regional-scale reduction of anthropogenic CO_2 emissions during the COVID-19 pandemic can be detected using space-based observations of atmospheric CO_2. For this purpose, we have analysed a small ensemble of satellite retrievals of column-averaged dry-air mole fractions of CO_2, i.e. XCO_2. We focus on East China because COVID-19 related CO_2 emission reductions are expected to be largest there early in the pandemic. We analysed four XCO_2 data products from the satellites Orbiting Carbon Observatory-2 (OCO-2) and Greenhouse gases Observing SATellite (GOSAT). We use a data-driven approach that does not rely on *a priori* information about CO_2 sources and sinks and ignores atmospheric transport. Our approach utilises the computation of XCO_2 anomalies, ΔXCO_2, from the satellite Level 2 data products using a method called DAM (Daily Anomalies via (latitude band) Medians). DAM removes large-scale, daily XCO_2 background variations, yielding XCO_2 anomalies that correlate with the location of major CO_2 source regions such as East China. We analysed satellite data between January 2015 and May 2020 and compared monthly XCO_2 anomalies in 2020 with corresponding monthly XCO_2 anomalies of previous years. In order to link the XCO_2 anomalies to East China fossil fuel (FF) emissions, we used XCO_2 and corresponding FF emissions from NOAA's (National Oceanic and Atmospheric Administration) CarbonTracker version CT2019 from 2015 to 2018. Using this CT2019 data set,

https://doi.org/10.5194/amt-2020-386
Preprint. Discussion started: 8 October 2020

Atmospheric Measurement Techniques Discussions

we found that the relationship between target region ΔXCO_2 and the FF emissions of the target region is approximately linear and we quantified slope and offset via a linear fit. We use the empirically obtained linear equation to compute ΔXCO_2^{FF}, an estimate of the target region FF emissions, from the satellite-derived XCO_2 anomalies, ΔXCO_2. We focus on October to May periods to minimize contributions from biospheric carbon fluxes and quantified the error of our FF estimation method for this period by applying it to CT2019. We found that the difference of the retrieved FF emissions and the CT2019 FF emissions in terms of the root-mean-square-error (RMSE) is 0.39 $GtCO_2$/year (4%). We applied our method to NASA's (National Aeronautics and Space Administration) OCO-2 XCO_2 data product (version 10r) and to three GOSAT products. We focus on estimates of the relative change of East China monthly emissions in 2020 relative to previous months. Our results show considerable month-to-month variability (especially for the GOSAT products) and significant differences across the ensemble of satellite data products analysed. The ensemble mean indicates emission reductions by approximately 8% ± 10% in March 2020 and 10% ± 10% in April 2020 (uncertainties are 1-sigma) and somewhat lower reductions for the other months in 2020. Using only the OCO-2 data product, we obtain smaller reductions of 1-2% (depending on month) with an uncertainty of ±2%. The large uncertainty and the differences of the results obtained for the individual ensemble members indicates that it is challenging to reliably detect and to accurately quantify the emission reduction. There are several reasons for this including the weak signal (the expected regional XCO_2 reduction is only on the order of 0.1-0.2 ppm), the sparseness of the satellite data, remaining biases and limitations of our relatively simple data-driven analysis approach. Inferring COVID-19 related information on regional-scale CO_2 emissions using current satellite XCO_2 retrievals likely requires, if at all possible, a more sophisticated analysis method including detailed transport modelling and considering *a priori* information on anthropogenic and natural CO_2 surface fluxes.

1 Introduction

Carbon dioxide (CO_2) is the most important anthropogenic greenhouse gas significantly contributing to global warming (IPCC, 2013). CO_2 has many natural and anthropogenic sources and sinks and our current understanding of them has significant gaps (e.g., Reuter et al., 2017c; Friedlingstein et al., 2019). Efforts are ongoing to improve the fundamental understanding of the global carbon cycle, to improve our ability to project future changes, and to verify the effectiveness of policies such as the Paris Agreement (https://unfccc.int/process-and-meetings/the-paris-agreement/the-paris-agreement, last access: 8-Sept-2020) aiming to reduce greenhouse gas emissions (e.g., Ciais et al., 2014, 2015; Pinty et al., 2017, 2019; Crisp et al., 2018; Matsunaga and Maksyutov, 2018; Janssens-Maenhout et al., 2020).

Retrievals of XCO_2 from the satellite sensors SCIAMACHY/ENVISAT (Burrows et al., 1995; Bovensmann et al., 1999; Reuter et al., 2010, 2011), TANSO-FTS/GOSAT (Kuze et al., 2016) and from the Orbiting Carbon Observatory-2 (OCO-2) satellite (Crisp et al., 2004; Eldering et al., 2017; O'Dell et al., 2012, 2018) have been used in recent years to obtain information on natural CO_2 sources and sinks (e.g., Basu et al., 2013; Chevallier et al., 2014, 2015; Reuter et al., 2014a, 2017c; Schneising et al., 2014; Houweling et al., 2015; Kaminski et al., 2017; Liu et al., 2017; Eldering et al., 2017; Yin et al., 2018; Palmer et

https://doi.org/10.5194/amt-2020-386
Preprint. Discussion started: 8 October 2020


Atmospheric Measurement Techniques Discussions

al., 2019; Miller and Michalak, 2020), on anthropogenic CO_2 emissions (e.g., Schneising et al., 2008, 2013; Reuter et al., 2014b, 2019; Nassar et al., 2017; Schwandner et al., 2017; Matsunaga and Maksyutov, 2018; Miller et al., 2019; Labzovskii et al., 2019; Wu et al., 2020; Zheng et al., 2020a; Ye et al., 2020) and for other applications such as climate model assessments (e.g., Lauer et al., 2017; Gier et al., 2020) or data assimilation (e.g., Massart et al., 2016).

Here we use an ensemble of satellite retrievals of XCO_2 to determine whether COVID-19 related regional-scale CO_2 emission reductions can be detected and quantified using the current space-based observing system. This is important in order to establish the capabilities of current satellites, which have been optimized to obtain information on natural carbon sources and sinks, but not to obtain information on anthropogenic emissions. Nevertheless, data from existing satellites have already been used to assess anthropogenic emissions (see publications cited above). These assessments and the assessment presented in this publication are relevant for future satellites focussing on anthropogenic emissions such as the planned European Copernicus Anthropogenic CO_2 Monitoring (CO2M) mission (e.g., ESA, 2019; Kuhlmann et al., 2019; Janssens-Maenhout et al., 2020), which is based on the CarbonSat concept (Bovensmann et al., 2010; Velazco et al., 2011; Buchwitz et al., 2013; Pillai et al., 2016; Broquet et al., 2018).

We focus on China because regional-scale COVID-19 related CO_2 emission reductions are expected to be largest there early in the pandemic (Le Quéré et al., 2020; Liu et al., 2020). Satellite data have been used to estimate China's CO_2 emissions during the COVID-19 pandemic (Zheng et al., 2020b), but that study inferred CO_2 reductions from retrievals of nitrogen dioxide (NO_2) not using XCO_2. Estimates of emission reductions have also been derived from bottom-up statistical assessments of fossil fuel use and other economic indicators. According to Le Quéré et al., 2020, China's CO_2 emissions decreased by 242 $MtCO_2$ (uncertainty range 108 – 394 $MtCO_2$) during January – April 2020. As China's annual CO_2 emissions are approximately 10 $GtCO_2$/year (Friedlingstein et al., 2019), i.e., approximately 3.3 $GtCO_2$ in a 4-month period assuming constant emissions, the average relative (COVID-19 related) change during January – April 2020 is therefore approximately 7% ± 4% (0.242/3.3 ± 0.14/3.3). This agrees reasonably well with the estimate reported in Liu et al., (2020), which is 10.3% for China during the first quarter of 2020 compared to the same period in 2019. Liu et al., (2020) also indicate some challenges in terms of interpreting CO_2 emission reductions as being caused by COVID-19, e.g., the fact that the first months of 2020 were exceptionally warm across much of the northern hemisphere. CO_2 emissions associated with home heating may have therefore been somewhat lower than for the same period in 2019, even without the disruption in economic activities and energy production caused by COVID-19 and related lockdowns.

Sussmann and Rettinger, 2020, studied grond-based remote sensing XCO_2 retrievals of the Total Carbon Column Observing Network (TCCON) to find out whether related atmospheric concentration changes may be detected by the TCCON and brought into agreement with bottom-up emission-reduction estimates. To the best of our knowledge, our study is the first attempt to determine quantitatively whether COVID-19 related regional-scale CO_2 emission reductions can be detected using existing space-based observations of XCO_2, although some qualitative results related to this application are also provided in the internet (e.g., ESA-NASA-JAXA, 2020). Regional-scale reductions of tropospheric NO_2 columns have been reported for

https://doi.org/10.5194/amt-2020-386
Preprint. Discussion started: 8 October 2020


Atmospheric Measurement Techniques Discussions

China (e.g., Zhang et al., 2020; Bauwens et al., 2020), but for CO_2 such an assessment is more challenging because of small XCO_2 changes on top of a large background. For example, over extended anthropogenic source areas such as East China, the XCO_2 enhancement due to anthropogenic emissions is typically only approximately 1 - 2 ppm (0.25% - 0.5% of 400 ppm) or even less (see, e.g., Schneising et al., 2008, 2013; Hakkarainen et al., 2016, 2019; and this study). A 10% emission reduction would therefore only change the regional XCO_2 enhancement by 0.1 to 0.2 ppm. This is below the single measurement precision of current satellite XCO_2 data products, which is about 1.8 ppm (1-sigma) (e.g., Dils et al., 2014; Kulawik et al., 2016; Buchwitz et al., 2015, 2017a; Reuter et al., 2020) for GOSAT and around 1 ppm for OCO-2 (Wunch et al., 2017; Reuter et al., 2019). This implies that the satellite data need to be averaged to reduce random error (noise) contributions. Therefore, we focus on XCO_2 monthly averages. The accuracy of the East China satellite XCO_2 retrievals averaged over monthly timescales is difficult to assess because of limited reference data. The validation of the satellite data products is primarily based on comparisons with ground-based XCO_2 retrievals from the TCCON, a relatively sparse network with an uncertainty of about 0.4 ppm (Wunch et al., 2010). The estimated precision and accuracy of the satellite XCO_2 retrievals as obtained from comparisons with TCCON XCO_2 retrievals is typically on the order of 0.7 ppm (e.g., Buchwitz et al., 2017a; Reuter et al., 2020) but this estimate assumes error-free TCCON retrievals, i.e., it neglects the non-negligible uncertainty of TCCON.

This manuscript is structured as follows: In Sect. 2 we present the satellite and model data used for this study and in Sect. 3 we present the analysis method. The main section is Sect. 4 where we present and discuss the results. A summary and conclusions are given in Sect. 5.

2 Data

In this section, we present a short overview about the input data used for this study.

2.1 Satellite XCO_2 estimates

This study uses four satellite XCO_2 Level 2 (L2) data products. An overview about these data sets is provided in Tab. 1 including references and access information. The first product listed in Tab. 1 is the latest bias-corrected OCO-2 XCO_2 product delivered to the Goddard Earth Science Data and Information Services Center (GES DISC) by the OCO-2 team (ACOS v10r Lite). The other three satellite XCO_2 datasets are different versions of the GOSAT XCO_2 product derived using retrieval algorithms developed by groups at the University of Leicester, U.K. (UoL-FP v7.3), the Netherlands Institute for Space Research (RemoTeC v2.3.8), and the University of Bremen, Germany (FOCAL v1.0).

The XCO_2 estimates derived from OCO-2 and GOSAT observations are complementary because these two spacecraft use different sampling strategies. OCO-2 has been operating since September 2014. Its spectrometers collect about 85000 cloud-free XCO_2 soundings each day along a narrow (< 10 km) ground track as it orbits the Earth 14.5 times each day from its sun synchronous 1:36 PM orbit. The OCO-2 soundings provide continuous measurements with relatively high spatial resolution

https://doi.org/10.5194/amt-2020-386
Preprint. Discussion started: 8 October 2020


Atmospheric Measurement Techniques Discussions

(2.25 km) along each track, but the individual ground tracks are separated by almost 25° longitude in any given day. This spacing is reduced to approximately 1.5° longitude after a 16-day ground track repeat cycle. GOSAT has been returning 300 to 1000 cloud-free XCO_2 soundings each day since April 2009. Its TANSO-FTS spectrometer collects soundings with ~10.6 km diameter surface footprints, separated by approximately 250 km along and across its ground track at it orbits from north to south across the sunlit hemisphere.

2.2 Model CO_2 data

We use data from NOAA's (National Oceanic and Atmospheric Administration) CO_2 assimilation system, CarbonTracker (CT2019) (Jacobson et al., 2020; Peters et al., 2007) to define the relationship between XCO_2 anomalies and fossil fuel emissions. CarbonTracker is a global atmospheric inverse model that assimilates atmospheric CO_2 measurements as well as estimates of emissions from fossil fuels and fires and other sources into an atmospheric transport model to estimate emissions and uptake of CO_2 by the land biosphere and oceans. An overview about CT2019 set is provided in Tab. 2 including references and access information. A description of CT2019 can also found on the CT2019 website (https://www.esrl.noaa.gov/gmd/ccgg/carbontracker/index.php, last access: 24-September 2020): "CarbonTracker produces model predictions of atmospheric CO_2 mole fractions, to be compared with the observed atmospheric CO_2 mole fractions. The difference between them is attributed to differences in the sources and sinks used to make the prediction (the so-called 'first-guess') and the sources and sinks affecting the true atmospheric CO_2. Using numerical techniques, these differences are used to solve for a set of sources and sinks that most closely matches the observed CO_2 in the atmosphere. CarbonTracker has a representation of atmospheric transport based on weather forecasts, and modules representing air-sea exchange of CO_2, photosynthesis and respiration by the terrestrial biosphere, and release of CO_2 to the atmosphere by fires and combustion of fossil fuels."

3. Methods

To analyse the satellite data with respect to regionally elevated XCO_2 due to anthropogenic CO_2 emissions, we use a method referred to as DAM (Daily Anomalies via (latitude band) Medians). The DAM method is essentially identical with the method described in Hakkarainen et al., 2016 and 2019. They applied their method to the OCO-2 Level 2 XCO_2 data product to filter out trends and seasonal variations in order to isolate CO_2 source/sink signals. Hakkarainen et al., 2019, explain their method as follows: "In order to obtain the background, we calculate the daily medians for each 10-degree latitude band and linearly interpolate the resulting values to each OCO-2 data point. The median was chosen because it better represents the typical value in each latitude band, and it is not skewed towards extreme values". Our approach is very similar, but instead of interpolation, we compute the median around each latitude ("running median") using a latitude band width of ±15 deg. We use a larger width compared to Hakkarainen et al., 2019, because we also apply our method to GOSAT data, which are much sparser than OCO-2 data. Our investigations showed that the width of the latitude band is not critical but needs to be

https://doi.org/10.5194/amt-2020-386
Preprint. Discussion started: 8 October 2020


Atmospheric Measurement Techniques Discussions

wide enough to contain a statistically significant sample, but narrow enough to resolve large latitudinal gradients in CO_2. We subtract the corresponding median from each single XCO_2 observation as contained in the original Level 2 XCO_2 data product files to obtain a data set of XCO_2 anomalies, ΔXCO_2. For illustration, we gridded these anomalies to obtain global maps. Figure 1 shows such a DAM XCO_2 anomaly map at $1^o x 1^o$ resolution covering the time period 2015 – 2019. The resulting spatially resolved XCO_2 anomalies are very similar as the one shown in Hakkarainen et al., 2019 (see their Fig. 3, top panel). The good agreement confirms the finding reported above that the generation of these anomaly maps does not critically depend on how exactly the median is computed and used to subtract "the background".

A zoom into Fig. 1 is presented in Fig. 2, which shows more details for China and surrounding areas. As can be seen from Fig. 2, the DAM ΔXCO_2 has a positive anomaly especially in the region between Beijing, Wuhan and Hong Kong with highest values in the area between Beijing and Shanghai. This positive anomaly indicates that this region is an important CO_2 source region. Of course, there is no one-to-one correspondence (especially not for every grid cell) between these XCO_2 anomalies and local CO_2 emissions (or uptake) because the emitted CO_2 is transported and mixed in the atmosphere. Furthermore, the satellite data are typically sparse due to strict quality filtering to avoid potential XCO_2 biases, for example, due to the presence of clouds. Cloud contaminated ground scenes are identified to the extent possible via the corresponding retrieval algorithm and flagged to be "bad" (see references listed in Tab. 1) and are therefore not used for this analysis. The sparseness of the satellite data set is obvious from Fig. 3, which shows DAM XCO_2 anomaly maps for the month of February during the six years from 2015 to 2020.

The geographical coordinates of the East China target region investigated here are listed in Tab. 3. The fossil fuel (FF) CO_2 emissions of this target region are approximately 8 $GtCO_2$/year, i.e., the selected target region covers approximately 80% of the FF emissions of entire China, which are approximately 10 $GtCO_2$/year (Le Quéré et al., 2018; Friedlingstein et al., 2019). For our East China analysis, we compute regional averages of DAM XCO_2 anomalies by averaging the ΔXCO_2 values for all satellite ground scenes (footprints) as located in the East China target region for each day in the period January 2015 to May 2020. These East China daily time series are then further averaged to obtain monthly East China ΔXCO_2 as presented in the following section.

4. Results and discussion

4.1 Application of the DAM method to model data

To determine whether satellite XCO_2 retrievals can provide information on relative changes of anthropogenic CO_2 emissions for the East China target region, we must establish the relationship between the DAM XCO_2 anomalies (see Sect. 3) and the target region fossil fuel (FF) emissions. For this purpose, we use the CarbonTracker (CT2019) data set described in Sect. 2.2.

https://doi.org/10.5194/amt-2020-386
Preprint. Discussion started: 8 October 2020


Atmospheric Measurement Techniques Discussions

Figure 4 shows CT2019 XCO_2 maps (left) and corresponding surface CO_2 flux maps (right) for selected days in the January to May 2018 period. The model data are sampled at local noon, which is close to the overpass time of the satellite data sets used here. As can be seen from Fig. 4, XCO_2 is clearly elevated over the East China target region (red rectangle) relative to its surrounding region on 15-January-2018 (panel (a)) and on 15-March-2018 (panel (c)). On 15-May-2018 (panel (e)) the target region and parts of the surrounding region contain large areas of lower than average XCO_2, a pattern which primarily results from carbon uptake by vegetation during the growing season, which starts around May each year. The CO_2 fluxes, which are shown in the right-hand side panels of Fig. 4, show similar spatial pattern as the XCO_2 maps but as already explained, there is not a one-to-one correspondence between atmospheric XCO_2 and surface emissions due to atmospheric transport. The CO_2 fluxes are the sum of several contributing fluxes including FF emissions, biospheric fluxes and other fluxes (e.g., due to fires and the oceans).

Figure 5 shows time series obtained by applying the DAM method to CT2019 XCO_2 for the East China target region. The top panel shows the CT2019 FF emissions as thick red line. For each day, the DAM method was applied to CT2019 XCO_2 to compute daily (and then monthly) XCO_2 anomalies, ΔXCO_2. The monthly CT2019 ΔXCO_2 values were linearly fitted to the monthly CT2019 FF emissions to obtain a quantity referred to as ΔXCO_2^{FF}, which closely resembles the FF emissions as shown in the top panel of Fig. 5. The linear fit yields $\Delta XCO_2^{FF} = 0.914 \times \Delta XCO_2 + 7.106$, with ΔXCO_2 in parts per million (ppm) and ΔXCO_2^{FF} in $GtCO_2$/year. Using this linear transformation, ΔXCO_2 can be transformed into ΔXCO_2^{FF} and daily and monthly ΔXCO_2^{FF} values are shown in Fig. 5 as thin grey line and blue dots, respectively.

Initially, we assumed that ΔXCO_2 is directly proportional to the target region fossil fuel emissions, i.e., we assumed that FF is (approximately) equal to a constant multiplied by ΔXCO_2 (no offset added). If we were only interested in relative changes in emissions, we would not need the exact values of the scaling factor. We found that ΔXCO_2 is around 2 ppm for January but decreases in subsequent months, nearly approaching zero in May (not shown here but see Fig. 5, top panel, showing a time series of ΔXCO_2^{FF} (blue dots)). As anthropogenic emissions are not expected to change that much within a few months we concluded that the simple proportionality assumption does not hold. We then used the CT2019 data set to test our method. We applied our method to CT2019 XCO_2 and compared the retrieved FF values with the true FF values as used by CT2019. We found large differences which could be significantly reduced by adding an offset. To obtain numerical values for the offset (see parameter B in Fig. 5, top panel) and for the scaling factor (see parameter A in Fig. 5, top panel) we used a linear fit as explained above, i.e., these two parameters are obtained empirically.

We use target region monthly ΔXCO_2^{FF} as a satellite-based estimate of target region monthly FF emissions. The middle and the bottom panels of Fig. 5 show the absolute and the relative monthly differences between ΔXCO_2^{FF} and the FF emissions, respectively. Also listed are several quantities used to characterise the level of agreement/disagreement: D is the mean difference, S is the standard deviation of the difference, RMSE is the root-mean-square-error and R is the linear correlation coefficient of the monthly ΔXCO_2^{FF} and FF values. As can be seen, the RMSE is 0.45 $GtCO_2$/year (6%) for the entire time series 2015 – 2018. The RMSE is reduced to 0.39 $GtCO_2$/year (4%) if the analysis is restricted to time periods covered by the

https://doi.org/10.5194/amt-2020-386
Preprint. Discussion started: 8 October 2020


Atmospheric Measurement Techniques Discussions

months October to May, which is the relevant period for this study as it covers pre-COVID-19 (October – December 2019) and COVID-19 (January – May 2020) periods. Excluding June to September data reduces the RMSE because (during this summer period) disturbances from biospheric fluxes (i.e., photosynthesis related fluxes during the vegetation growing season) are largest. As shown in Fig. 5, ΔXCO_2^{FF} is to a good approximation proportional to FF emissions and for this study it is assumed that relative changes of the monthly ΔXCO_2^{FF} values can be used as a sufficiently accurate proxy for relative changes of the monthly FF emissions.

The method described in this section has been applied to convert satellite-derived target region XCO_2 anomalies, ΔXCO_2, into ΔXCO_2^{FF}. Monthly ΔXCO_2^{FF} values have been computed for each satellite data product and used to find out if FF reductions during the COVID-19 pandemic can be detected in these time series, as will be explained in the following sub-sections.

4.2 Application of the DAM method to satellite XCO_2 retrievals

The DAM method described in the previous section has been applied to a small ensemble of XCO_2 retrievals from OCO-2 and GOSAT (see details listed in Tab. 1) and the results are presented below. As noted above, a key difference between the OCO-2 and the GOSAT data products is the different sampling of the target region, with GOSAT having much sparser coverage compared to OCO-2. This is illustrated in Fig. 6, which shows February to March 2020 averages of the OCO-2 XCO_2 data product (Fig. 6a) and the three GOSAT data products (Fig. 6b – 6d) at 1^ox1^o resolution. The OCO-2 product shown in Fig. 6a is NASA's OCO-2 operational "Atmospheric CO_2 Observations from Space" (ACOS) algorithm version 10r bias corrected XCO_2 product (the so called Lite product), which is referred to in this publication via the product identifier (ID) CO2_OC2_ACOS. The three GOSAT XCO_2 products are (see details and references as given in Tab. 1): Fig. 6b: University of Leicester's GOSAT product (ID CO2_GOS_OCFP); Fig. 6c: SRON Netherlands Institute for Space Research GOSAT product (CO2_GOS_SRFP); Fig. 6d: University of Bremen's GOSAT product (CO2_GOS_FOCA) as retrieved with the "Fast atmOspheric traCe gAs retrievaL" (FOCAL) retrieval algorithm initially developed for OCO-2 (Reuter et al., 2017a, 2017b). As can be seen from Fig. 6, the spatial sampling of the target region is different for each product as only quality-filtered (i.e., "good") data are shown and the quality filtering is algorithm specific (see references listed in Tab. 1).

4.2.1 Application to NASA's OCO-2 (version 10r) XCO_2

Figure 7 shows the results obtained by applying the DAM method to product CO2_OC2_ACOS for the East China target region for the period January 2015 to May 2020. The top panel shows the daily DAM XCO_2 anomalies as thin grey line and the corresponding monthly averages as red dots. The amplitude (approximately ±1 ppm) and time dependence (e.g., there is a minimum in the middle of each year) is as expected as can be concluded from a comparison with the corresponding CT2019 results shown in Fig. 5 (but note that Fig. 7 shows ΔXCO_2 whereas Fig. 5 shows ΔXCO_2^{FF}, which differs somewhat in

https://doi.org/10.5194/amt-2020-386
Preprint. Discussion started: 8 October 2020


Atmospheric Measurement Techniques Discussions

amplitude and offset due to the applied linear transformation as explained in Sect. 4.1). Two criteria need to be fulfilled for the monthly data shown in this figure: (i) The minimum number of days per month is 5 and (ii) the minimum number of observations per day is 30, i.e., at least 5 days per month having (for each day) at least 30 observations per day in the target region need to be available for a month to be accepted (results for other combinations of these two parameters are presented below).

The middle panel of Fig. 7 shows monthly ΔXCO_2^{FF} for October - May for five different periods: October 2019 – May 2020 (red), October 2018 – May 2019 (blue) and three corresponding periods in earlier years (see annotation as listed in the figure panel). As can be seen from this panel, the red curve (October 2019 – May 2020) shows, apart from March 2020, somewhat lower values in the period February 2020 – May 2020 (i.e., during the "COVID-19 period") compared to January 2020 and earlier months ("pre-COVID-19 period"). However, the time dependence shows significant month-to-month variability. Furthermore, a similar time dependency is also present for October 2015 – May 2016 (pink). In comparison to the other periods from earlier years, the (red) October 2019 – May 2020 values are mostly close to the maximum (or even exceed) the values of the other curves corresponding to earlier October – May time periods.

The bottom panel of Figure 7 shows the corresponding relative differences, as we are mostly interested in relative (percentage) changes of the target region FF emissions. The blue dots (and connecting lines) show the relative difference between the red dots from in the middle panel (this time series ends in May 2020) and the blue dots shown in the middle panel (this time series ends in May 2019). If for simplicity we refer to time series ending in May as "2020" (red dots in middle panel) and "2019" (blue dots in middle panel), then the blue dots displayed in the bottom panel show "(2020-2019)/2019", i.e., they are a proxy for the relative change of the target region FF emissions of the corresponding months in 2020 relative to 2019 (for January to May; for October to December the difference corresponds to 2019 relative to 2018). The green dots show the corresponding relative differences for 2020 relative to 2018, the orange dots correspond to the relative differences for 2020 relative to 2017 and the pink dots show the relative differences for 2020 relative to 2016. As can be seen from the bottom panel of Fig. 7, the relative difference between the time series ending in May 2020 and in May 2019 (blue dots in the bottom panel) also shows significant variability from month to month. Compared to all previous differences (2020-2018, 2020-2017, etc.) one sees that these differences are mostly positive and typically somewhere in the range between 0% and +10%. Figure 7 indicates that during October 2019 to May 2020 target region FF emissions are on average a few percent higher compared to previous years.

The data shown in the bottom panel of Fig. 7 are also shown in Fig. 8 (see thin lines using different colours) but together with derived monthly median (and mean) values. In addition, vertical bars are shown to indicate the scatter of the monthly values. As we are primarily interested in changes during the January to May 2020 period compared to preceding months (October – December 2019) and compared to previous years, the median has been computed for each month and the October – December 2019 (i.e., pre-COVID-19 OND months) mean value has been subtracted to highlight the difference of 2020 relative to 2019.

https://doi.org/10.5194/amt-2020-386
Preprint. Discussion started: 8 October 2020


Atmospheric Measurement Techniques Discussions

The corresponding monthly medians are shown as thick royal blue symbols (and connecting lines) and the scatter - as computed from the standard deviation of the monthly values – is shown as royal blue vertical bars. The light blue symbols and lines show the corresponding values when using the mean instead of the median. In grey, the "original" median values are shown, i.e., in grey, the median values are shown before the offset has been subtracted (i.e., the "absolute" values are shown in grey and the corresponding "OND anomaly" is shown in royal blue). The royal blue curve indicates that ΔXCO_2^{FF}, our proxy for the target region FF emissions, is 2-3% lower in February to April 2020 compared to October to December 2019 and earlier years. Due to the large scatter and significant month-to-month variability and possibly also for other reasons (e.g., the unusual meteorological conditions in the first few months of 2020, see, for example, Liu et al., 2020) it is unclear to what extent this reduction is related to COVID-19 countermeasures.

Figures 7 and 8 have been generated with the requirement that, for each day, at least 30 observations need to be available in the target region and that for each month, at least 5 days fulfilling this 30 observations/day requirement are available. Figure 9 is similar to Fig. 8 except that results for additional combinations of minimum number of observations per day and minimum number of days per month have been added. Here, the results depend somewhat on which combination of these parameters is used, but the overall end result as shown via the royal blue symbols and lines is fairly stable as it depends only marginally on which set of combinations is used as can be seen when comparing Fig. 9 with Fig. 8.

4.2.2 Application to GOSAT XCO_2 data products

The same analysis method as applied to NASA's OCO-2 data product (see Sect. 4.2.1) has also been applied to the three GOSAT XCO_2 data products listed in Tab. 1. The results are shown in Fig. 10 for product CO2_GOS_OCFP, in Fig. 11 for product CO2_GOS_SRFP, and in Fig. 12 for product CO2_GOS_FOCA.

The month-to-month variations are larger for these products compared to product CO2_OC2_ACOS (e.g., Figs. 9; note the different scales of the y-axes). This is very likely because GOSAT products are sparse compared to the OCO-2 product (see Fig. 6) but also because the single observation random error (precision) is larger for GOSAT.

https://doi.org/10.5194/amt-2020-386
Preprint. Discussion started: 8 October 2020


Atmospheric Measurement Techniques Discussions

Analysis of product CO2_GOS_OCFP (Fig. 10) suggests that on average, emissions are reduced in 2020 (approximately -12% ± 12%) but strong conclusions cannot be drawn because of large uncertainty (approximately 12%, 1-sigma). Product CO2_GOS_SRFP (Fig. 11) shows no clear time dependence due to large month-to-month variability and the same seems to be true for product CO2_GOS_FOCA (Fig. 12).

4.2.3 Ensemble mean and uncertainty

An overview about the results obtained from all four satellite data products is shown in Fig. 13. The results obtained from the individual products (as shown in royal blue in Figs. 9 - 12) are shown here using reddish colours (the corresponding numerical values are listed in Tab. 4). Also shown in Fig. 13 is the mean of the ensemble members and its estimated uncertainty (in dark blue); the corresponding numerical values are listed in the bottom row of Tab. 4. In Fig. 13, the ensemble mean shows on average slightly lower values during March and April 2020 compared to the other months, suggesting an emission reduction by several percent (-8% in March and -10% in April). However, the 1-sigma uncertainties shown as dark blue vertical lines are large (±10%) and typically overlap with the zero, i.e., no change, line. Furthermore, as already discussed, there are considerable month-to-month variations and large differences between the results obtained from the individual satellite data products. It is therefore concluded that the expected reduction cannot be accurately quantified.

5 Summary and conclusions

We have analysed a small ensemble of retrieved satellite XCO_2 data products to investigate whether a regional-scale reduction of atmospheric CO_2 during the COVID-19 pandemic can be detected over East China. Specifically, we analysed four XCO_2 data products from the satellites OCO-2 and GOSAT. For this purpose, we used a data-driven approach, which involves the computation of XCO_2 anomalies, ΔXCO_2, using a method called DAM (Daily Anomalies via (latitude band) Medians). This method, which is essentially identical with the method developed at Finnish Meteorological Institute (FMI, Hakkarainen et al., 2019), helps to isolate local or regional XCO_2 enhancements originating from anthropogenic CO_2 emissions from large-scale daily XCO_2 background variations. We analysed satellite data between January 2015 to May 2020 and compared year 2020 monthly XCO_2 anomalies with the corresponding monthly XCO_2 anomalies from previous months.

In order to link the satellite-derived XCO_2 anomalies to East China fossil fuel (FF) emissions, we used output from NOAA's CO_2 assimilation system CarbonTracker (CT2019). Using CT2019, we show that ΔXCO_2 can be linearly transformed to "FF

https://doi.org/10.5194/amt-2020-386
Preprint. Discussion started: 8 October 2020


Atmospheric Measurement Techniques Discussions

related XCO_2 enhancements", denoted ΔXCO_2^{FF}, and via a linear fit we established a linear empirical equation to relate these two quantities. We use this empirical equation to compute ΔXCO_2^{FF}, an estimate of the target region FF emissions, from the satellite-derived XCO_2 anomalies, ΔXCO_2. We focus on October to May periods and found using CT2019 that the root-mean-square-error (RMSE) of our FF estimation method is approximately 0.39 $GtCO_2$/year (4%). These months are less affected by disturbances from natural terrestrial vegetation carbon fluxes (using all months the RMSE is larger, namely 0.45 $GtCO_2$/year or 6%) and appropriate as they cover relevant pre-COVID-19 (e.g., October – December 2019) and COVID-19 (January – May 2020) periods. However, satellite retrievals during these months are more challenging because of the low sun angles and cloudiness.

We applied our method to each of the four satellite XCO_2 data products and computed monthly ΔXCO_2^{FF} for East China ("retrieved East China monthly FF emissions"). Our results show considerable month-to-month variability (especially for the GOSAT products) and significant differences across the ensemble of satellite data products analysed. The ensemble mean suggests emission reductions by approximately 8% ± 10% in March 2020 and 10% ± 10% in April 2020 (uncertainties are 1-sigma) and somewhat lower reductions for the other months in 2020. These values are dominated by the GOSAT ensemble members. Analysis of the OCO-2 product yields smaller values showing a reduction of 1-2% with an uncertainty of ±2%.

The large uncertainty, which is on the order of the derived reduction (i.e., 100%, 1-sigma), and the large spread of the results obtained for the individual ensemble members, indicates that it is challenging to reliably detect and to accurately quantify the emission reduction using the current generation of space based methods and the simple DAM analysis strategy adopted here. These findings are not unexpected. Fossil fuel emissions related regional XCO_2 enhancements are typically only 1 to 2 ppm and even a 10% emission reduction would therefore only correspond to a reduction of the fossil fuel related regional XCO_2 enhancement by 0.1 to 0.2 ppm. XCO_2 variations as small as 0.2 ppm are below the estimated uncertainty of the single footprint satellite XCO_2 retrievals. This single observations uncertainty, which is around 0.7 ppm (e.g., Buchwitz et al., 2017a; Reuter et al., 2020), has been obtained by comparisons with ground-based Total Carbon Column Observing Network (TCCON) XCO_2 retrievals, which have an uncertainty of 0.4 ppm (1-sigma, Wunch et al., 2010). To reduce random errors, we use monthly averaged data. Averaging results in reducing the random error but investigations have shown that random errors do not simply scale with the inverse of the square root of number of observations added (Kulawik et al., 2016).

We conclude that inferring COVID-19 related information on regional-scale CO_2 emissions using current (quite sparse) satellite XCO_2 retrievals requires, if at all possible, a more sophisticated analysis method including the use of detailed *a priori* information and atmospheric transport modelling.

The extent to which COVID-19 related emission reductions can be resolved on smaller scales - such as power plants or cities (e.g., Nassar et al., 2017; Reuter et al., 2019; Zheng et al., 2020a; Wu et al., 2020) has not yet been investigated in detail (to the best of our knowledge). For this purpose, XCO_2 retrievals from NASA's OCO-3 mission are also very promising, especially because of its Snapshot Area Map (SAM) mode, which permits the mapping of XCO_2 over ~80 km by 80 km areas around

https://doi.org/10.5194/amt-2020-386
Preprint. Discussion started: 8 October 2020


Atmospheric Measurement Techniques Discussions

localized anthropogenic CO_2 emission sources (see https://ocov3.jpl.nasa.gov/ (last access: 28-Aug-2020)). Even more complete coverage is planned for the Copernicus CO2M mission in the future (e.g., Janssens-Maenhout et al., 2020).

375

https://doi.org/10.5194/amt-2020-386
Preprint. Discussion started: 8 October 2020


Atmospheric Measurement Techniques Discussions

Acknowledgements

This study has been funded in parts by the European Space Agency (ESA) via projects ICOVAC (Impacts of COVID-19 lockdown measures on Air quality and Climate) and GHG-CCI+ (http://cci.esa.int/ghg, last access: 13-August-2020) and the University and the State of Bremen. We acknowledge financial support for the generation of several data sets used as input for this study: (i) European Commission via Copernicus Climate Change Service (C3S, https://climate.copernicus.eu/, last access: 22-July-2020) project C3S_312b_Lot2, (ii) the Japanese space agency JAXA (contract 19RT000692) and (iii) EUMETSAT (contract EUM/CO/19/4600002372/RL). H.Boe., Univ. Leicester, was funded as part of NERC's support of the National Centre for Earth Observation (NE/R016518/1).

We also acknowledge access to OCO-2 XCO_2 data product "OCO2_L2_Lite_FP 10r" obtained from NASA's Earthdata GES DISC website (https://disc.gsfc.nasa.gov/datasets?keywords=OCO-2%20v10r&page=1 (last access: 15-Aug-2020)).

We thank JAXA and the National Institute for Environmental Studies (NIES), Japan, for access to GOSAT Level 1 (L1) data and ESA for making the GOSAT L1 products available via the ESA Third Party Mission (TPM) archive.

We acknowledge CarbonTracker CT2019 results provided by NOAA ESRL, Boulder, Colorado, USA, from the website at http://carbontracker.noaa.gov (last access: 22-July-2020). We also acknowledge feedback from Andy Jacobson on an early draft of this manuscript.

Some of the work reported here was conducted by the Jet Propulsion Laboratory, California Institute of Technology under contract to NASA. Government sponsorship is acknowledged.

Author contributions

M.B. designed the study, performed the analysis and led the writing of this paper in close cooperation with M.R., S.N., B.F.A., H.B., J.P.B., O.S. K.B. and M.H. Input data and corresponding advice has been provided by M.R., S.N., A.D.N., H.Boe., L.W, J. L., I.A., C.W.O'D. and D.C. All authors contributed to significantly improve the manuscript.

Data availability. The key results of this study are listed in this manuscript in numerical form (Tab. 4). Access information for the satellite data used as input for this study is provided in Tab. 1. The CT2019 data are available from NOAA (see access information given in Tab. 2).

Competing financial interests

The authors declare no competing financial interests.

https://doi.org/10.5194/amt-2020-386
Preprint. Discussion started: 8 October 2020


Atmospheric Measurement Techniques Discussions

405

References

Basu, S., Guerlet, S., Butz, A., Houweling, S., Hasekamp, O., Aben, I., Krummel, P., Steele, P., Langenfelds, R., Torn, M., Biraud, S., Stephens, B., Andrews, A., and Worthy, D.: Global CO_2 fluxes estimated from GOSAT retrievals of total column CO_2, Atmos. Chem. Phys., 13, 8695–8717, doi:10.5194/acp-13-8695-2013, 2013.

Boesch, H., Anand, J., and Di Noia, A.: Product User Guide and Specification (PUGS) – ANNEX A for products CO2_GOS_OCFP, CH4_GOS_OCFP & CH4_GOS_OCPR (v7.2, 2009-2018), 3-Nov-2019, pp. 33, http://wdc.dlr.de/C3S_312b_Lot2/Documentation/GHG/PUGS/C3S_D312b_Lot2.3.2.3-v1.0_PUGS-GHG_ANNEX-A_v3.1.pdf (last access: 17-Aug-2020), 2019.

Bovensmann, H., Burrows, J. P., Buchwitz, M., Frerick, J., Noël, S., Rozanov, V. V., Chance, K. V., and Goede, A. H. P.: SCIAMACHY - Mission objectives and measurement modes, J. Atmos. Sci., 56 (2), 127-150, 1999.

Bovensmann, H., M. Buchwitz, J. P. Burrows, M. Reuter, T. Krings, K. Gerilowski, O. Schneising, J. Heymann, A. Tretner, and J. Erzinger, A remote sensing technique for global monitoring of power plant CO_2 emissions from space and related applications, Atmos. Meas. Tech., 3, 781-811, 2010.

Broquet, G., F.-M. Breon, E. Renault, M. Buchwitz, M. Reuter, H. Bovensmann, F. Chevallier, L. Wu, and P. Ciais, The potential of satellite spectro-imagery for monitoring CO_2 emissions from large cities, Atmos. Meas. Tech., 11, 681-708, https://doi.org/10.5194/amt-11-681-2018, 2018.

Buchwitz, M., Reuter, M., Bovensmann, H., Pillai, D., Heymann, J., Schneising, O., Rozanov, V., Krings, T., Burrows, J. P., Boesch, H., Gerbig, C., Meijer, Y., and Loescher, A.: Carbon Monitoring Satellite (CarbonSat): assessment of atmospheric CO_2 and CH_4 retrieval errors by error parameterization, Atmos. Meas. Tech., 6, 3477-3500, 2013.

Buchwitz, M., Reuter, M., Schneising, O., Boesch, H., Guerlet, S., Dils, B., Aben, I., Armante, R., Bergamaschi, P., Blumenstock, T., Bovensmann, H., Brunner, D., Buchmann, B., Burrows, J. P., Butz, A., Chédin, A., Chevallier, F., Crevoisier, C. D., Deutscher, N. M., Frankenberg, C., Hase, F., Hasekamp, O. P., Heymann, J., Kaminski, T., Laeng, A., Lichtenberg, G., De Mazière, M., Noël, S., Notholt, J., Orphal, J., Popp, C., Parker, R., Scholze, M., Sussmann, R., Stiller, G. P., Warneke, T., Zehner, C., Bril, A., Crisp, D., Griffith, D. W. T., Kuze, A., O'Dell, C., Oshchepkov, S., Sherlock, V., Suto, H., Wennberg, P., Wunch, D., Yokota, T., and Yoshida, Y.: The Greenhouse Gas Climate Change Initiative (GHG-CCI): comparison and quality assessment of near-surface-sensitive satellite-derived CO_2 and CH_4 global data sets, Remote Sensing of Environment, 162, 344-362, doi:10.1016/j.rse.2013.04.024, 2015.

Buchwitz, M., Reuter, M., Schneising, O., Hewson, W., Detmers, R. G., Boesch, H., Hasekamp, O. P., Aben, I., Bovensmann, H., Burrows, J. P., Butz, A., Chevallier, F., Dils, B., Frankenberg, C., Heymann, J., Lichtenberg, G., De Maziere, M., Notholt, J., Parker, R., Warneke, T., Zehner, C., Griffith, D. W. T., Deutscher, N. M., Kuze, A., Suto, H., and

https://doi.org/10.5194/amt-2020-386
Preprint. Discussion started: 8 October 2020


Atmospheric Measurement Techniques Discussions

Wunch, D.: Global satellite observations of column-averaged carbon dioxide and methane: The GHG-CCI XCO_2 and XCH_4 CRDP3 data set, Remote Sensing of Environment 203, 276-295, http://dx.doi.org/10.1016/j.rse.2016.12.027, 2017a.

Buchwitz, M., Schneising, O., Reuter, M., Heymann, J., Krautwurst, S., Bovensmann, H., Burrows, J. P., Boesch, H., Parker, R. J., Somkuti, P., Detmers, R. G., Hasekamp, O. P., Aben, I., Butz, A., Frankenberg, C., Turner, A. J., Satellite-derived methane hotspot emission estimates using a fast data-driven method, Atmos. Chem. Phys., 17, 5751-5774, doi:10.5194/acp-17-5751-2017, 2017b.

Buchwitz, M., Reuter, M., Schneising, O., Noel, S., Gier, B., Bovensmann, H., Burrows, J. P., Boesch, H., Anand, J., Parker, R. J., Somkuti, P., Detmers, R. G., Hasekamp, O. P., Aben, I., Butz, A., Kuze, A., Suto, H., Yoshida, Y., Crisp, D., and O'Dell, C.: Computation and analysis of atmospheric carbon dioxide annual mean growth rates from satellite observations during 2003-2016, Atmos. Chem. Phys., 18, 17355-17370, https://doi.org/10.5194/acp-18-17355-2018, 2018.

Burrows, J. P., Hölzle, E., Goede, A. P. H., Visser, H., and Fricke, W.: SCIAMACHY—Scanning Imaging Absorption Spectrometer for Atmospheric Chartography, Acta Astronaut., 35(7), 445–451, doi:10.1016/0094-5765(94)00278-t, 1995.

Butz, A., Guerlet, S., Hasekamp, O., Schepers, D., Galli, A., Aben, I., Frankenberg, C., Hartmann, J.-M., Tran, H., Kuze, A., Keppel-Aleks, G., Toon, G., Wunch, D., Wennberg, P., Deutscher, N., Griffith, D., Macatangay, R., Messerschmidt, J., Notholt, J., and Warneke, T.: Toward accurate CO_2 and CH_4 observations from GOSAT, Geophys. Res. Lett., doi:10.1029/2011GL047888, 2011.

Chevallier, F.: On the parallelization of atmospheric inversions of CO_2 surface fluxes within a variational framework, Geosci. Model. Dev., 6, 783-790, doi:10.5194/gmd-6-783-2013, 2013.

Chevallier, F., Palmer, P. I., Feng, L., Boesch, H., O'Dell, C. W., and Bousquet, P.: Towards robust and consistent regional CO_2 flux estimates from in situ and space-borne measurements of atmospheric CO_2, Geophys. Res. Lett., 41, 1065–1070, doi:10.1002/2013GL058772, 2014.

Chevallier, F.: On the statistical optimality of CO_2 atmospheric inversions assimilating CO_2 column retrievals, Atmos. Chem. Phys., 15, 11133–11145, https://doi.org/10.5194/acp-15-11133-2015, 2015.

Ciais, P., Dolman, A. J., Bombelli, A., Duren, R., Peregon, A., Rayner, P. J., Miller, C., Gobron, N., Kinderman, G., Marland, G., Gruber, N., Chevallier, F., Andres, R. J., Balsamo, G., Bopp, L., Bréon, F.-M., Broquet, G., Dargaville, R., Battin, T. J., Borges, A., Bovensmann, H., Buchwitz, M., Butler, J., Canadell, J. G., Cook, R. B., DeFries, R., Engelen, R., Gurney, K. R., Heinze, C., Heimann, M., Held, A., Henry, M., Law, B., Luyssaert, S., Miller, J., Moriyama, T., Moulin, C., Myneni, R. B., Nussli, C., Obersteiner, M., Ojima, D., Pan, Y., Paris, J.-D., Piao, S. L., Poulter, B., Plummer, S., Quegan, S., Raymond, P., Reichstein, M., Rivier, L., Sabine, C., Schimel, D., Tarasova, O., Valentini, R., Wang, R., van der Werf, G., Wickland, D., Williams, M., and Zehner, C.: Current systematic carbon-cycle observations and the need for implementing a policy-relevant carbon observing system, Biogeosciences, 11, 3547–3602, https://doi.org/10.5194/bg-11-3547-2014, 2014.

https://doi.org/10.5194/amt-2020-386
Preprint. Discussion started: 8 October 2020


Atmospheric Measurement Techniques Discussions

Ciais, P., Crisp, D., Denier van der Gon, H., Engelen, R., Janssens-Maenhout, G., Heimann, H., Rayner, P., and Scholze, M.: Towards a European Operational Observing System to Monitor Fossil CO_2 emissions, Final Report from the expert group, European Comission, October 2015, pp. 68, https://edgar.jrc.ec.europa.eu/news_docs/CO2_report_22-10-2015.pdf (last access: 26-Aug-2020), 2015.

Cogan, A. J., Boesch, H., Parker, R. J., Feng, L., Palmer, P. I., Blavier, J.-F. L., Deutscher, N. M., Macatangay, R., Notholt, J., Roehl, C., Warneke, T., and Wunsch, D.: Atmospheric carbon dioxide retrieved from the Greenhouse gases Observing SATellite (GOSAT): Comparison with ground-based TCCON observations and GEOS-Chem model calculations, J. Geophys. Res., 117, D21301, doi:10.1029/2012JD018087, 2012.

Crisp, D., Atlas, R. M., Bréon, F.-M., Brown, L. R., Burrows, J. P., Ciais, P., Connor, B. J., Doney, S. C., Fung, I. Y., Jacob, D. J., Miller, C. E., O'Brien, D., Pawson, S., Randerson, J. T., Rayner, P., Salawitch, R. S., Sander, S. P., Sen, B., Stephens, G. L., Tans, P. P., Toon, G. C.,Wennberg, P. O.,Wofsy, S. C., Yung, Y. L., Kuang, Z., Chudasama, B., Sprague, G.,Weiss, P., Pollock, R., Kenyon, D., and Schroll, S.: The Orbiting Carbon Observatory (OCO) mission, Advances in Space Research, 34, 700–709, 2004.

Crisp, D., Meijer, Y., Munro, R., Bowman, K., Chatterjee, A., Baker, D., Chevallier, F., Nassar, R., Palmer, P. I., Agusti-Panareda, A., Al-Saadi, J., Ariel, Y., Basu, S., Bergamaschi, P., Boesch, H., Bousquet, P., Bovensmann, H., Bréon, F.-M., Brunner, D., Buchwitz, M., Buisson, F., Burrows, J. P., Butz, A., Ciais, P., Clerbaux, C., Counet, P., Crevoisier, C., Crowell, S., DeCola, P. L., Deniel, C., Dowell, M., Eckman, R., Edwards, D., Ehret, G., Eldering, A., Engelen, R., Fisher, B., Germain, S., Hakkarainen, J., Hilsenrath, E., Holmlund, K., Houweling, S., Hu, H., Jacob, D., Janssens-Maenhout, G., Jones, D., Jouglet, D., Kataoka, F., Kiel, M., Kulawik, S. S., Kuze, A., Lachance, R. L., Lang, R., Landgraf , J., Liu, J., Liu, Y., Maksyutov, S., Matsunaga, T., McKeever, J., Moore, B., Nakajima, M., Natraj, V., Nelson, R. R., Niwa, Y., Oda, T., O'Dell, C. W., Ott, L., Patra, P., Pawson, S., Payne, V., Pinty, B., Polavarapu, S. M., Retscher, R., Rosenberg, R., Schuh, A., Schwandner, F. M., Shiomi, K., Su, W., Tamminen, J., Taylor, T. E., Veefkind, P., Veihelmann, B., Wofsy, S., Worden, J., Wunch, D., Yang, D., Zhang, P., and Zehner, C.: A CONSTELLATION ARCHITECTURE FOR MONITORING CARBON DIOXIDE AND METHANE FROM SPACE, Prepared by the CEOS Atmospheric Composition Virtual Constellation Greenhouse Gas Team, Committee on Earth Observation Satellites, Version 1.0, 8 October 2018, pp. 173, http://ceos.org/document_management/Meetings/Plenary/32/documents/CEOS_AC-VC_White_Paper_Version_1_20181009.pdf (last access: 26-Aug-2020), 2018.

Eldering, A., Wennberg, P. O., Crisp, D., Schimel, D. S., Gunson, M. R., Chatterjee, A., Liu, J., Schwandner, F. M., Sun, Y., O'Dell, C. W., Frankenberg, C., Taylor, T., Fisher, B., Osterman, G. B., Wunch, D., Hakkarainen, J., Tamminen, J., and Weir, B.: The Orbiting Carbon Observatory-2 early science investigations of regional carbon dioxide fluxes, Science, 358, eaam5745, doi: 10.1126/science.aam5745, 2017.

ESA, 2019: ESA, European Space Agency, Copernicus CO_2 Monitoring Mission Requirements Document, version 2.0 of 27/09/19, ESA Earth and Mission Science Division document ref. EOP-SM/3088/YM-ym, https://esamultimedia.esa.int/docs/EarthObservation/CO2M_MRD_v2.0_Issued20190927.pdf (last access: 15-July-2020), pp. 82, 2019.

ESA-NASA-JAXA, 2020: ESA, NASA and JAXA COVID-10 Dashboard (see: https://www.nasa.gov/coronavirus, https://www.nasa.gov/press-release/nasa-partner-space-agencies-amass-global-view-of-covid-19-impacts and/or https://www.esa.int/ESA_Multimedia/Images/2020/06/COVID-19_Earth_Observation_Dashboard2, last access: 15-July-2020).

Dils, B. Buchwitz, M., Reuter, M., Schneising, O., Boesch, H. , Parker, R., Guerlet, S., Aben, I., Blumenstock, T., Burrows, J. P., Butz, A., Deutscher, N. M., Frankenberg, C., Hase, F., Hasekamp, O. P., Heymann, J., De Maziere, M., Notholt, J., Sussmann, R., Warneke, T., Griffith, D., Sherlock, V., and Wunch, D.: The Greenhouse Gas Climate Change Initiative (GHG-CCI): comparative validation of GHG-CCI SCIAMACHY/ENVISAT and TANSO-FTS/GOSAT CO_2 and CH_4 retrieval algorithm products with measurements from the TCCON, Atmos. Meas. Tech., 7, 1723-1744, 2014.

Friedlingstein, P., Jones, M. W., O'Sullivan, M., Andrew, R. M., Hauck, J., Peters, G. P., Peters, W., Pongratz, J., Sitch, S., Le Quéré, C., Bakker, D. C. E., Canadell, J. G., Ciais, P., Jackson, R. B., Anthoni, P., Barbero, L., Bastos, A., Bastrikov, V., Becker, M., Bopp, L., Buitenhuis, E., Chandra, N., Chevallier, F., Chini, L. P., Currie, K. I., Feely, R. A., Gehlen, M., Gilfillan, D., Gkritzalis, T., Goll, D. S., Gruber, N., Gutekunst, S., Harris, I., Haverd, V., Houghton, R. A., Hurtt, G., Ilyina, T., Jain, A. K., Joetzjer, E., Kaplan, J. O., Kato, E., Klein Goldewijk, K., Korsbakken, J. I., Landschützer, P., Lauvset, S. K., Lefèvre, N., Lenton, A., Lienert, S., Lombardozzi, D., Marland, G., McGuire, P. C., Melton, J. R., Metzl, N., Munro, D. R., Nabel, J. E. M. S., Nakaoka, S. I., Neill, C., Omar, A. M., Ono, T., Peregon, A., Pierrot, D., Poulter, B., Rehder, G., Resplandy, L., Robertson, E., Rödenbeck, C., Séférian, R., Schwinger, J., Smith, N., Tans, P. P., Tian, H., Tilbrook, B., Tubiello, F. N., van der Werf, G. R., Wiltshire, A. J., and Zaehle, S.: Global Carbon Budget 2019, Earth Syst. Sci. Data, 11, 1783-1838, doi: 10.5194/essd-11-1783-2019, 2019.

Gier, B. K., Buchwitz, M., Reuter, M., Cox, P. M., Friedlingstein, P., and Eyring, V.: Spatially resolved evaluation of Earth system models with satellite column averaged CO_2, Biogeosciences Discuss., https://doi.org/10.5194/bg-2020-170, in review, 2020.

Hakkarainen, J., Ialongo, I., and Tamminen, J.: Direct space-based observations of anthropogenic CO_2 emission areas from OCO-2, Geophys. Res. Lett., 43, 11,400–11,406, doi:10.1002/2016GL070885, 2016.

Hakkarainen, J., Ialongo, I., Maksyutov, S., and Crisp, D.: Analysis of Four Years of Global XCO_2 Anomalies as Seen by Orbiting Carbon Observatory-2, Remote Sensing, 11, 850, doi:10.3390/rs11070850, pp. 20, 2019.

https://doi.org/10.5194/amt-2020-386
Preprint. Discussion started: 8 October 2020


Atmospheric Measurement Techniques Discussions

Houweling, S., Baker, D., Basu, S., Boesch, H., Butz, A., Chevallier, F., Deng, F., Dlugokencky, E. J., Feng, L., Ganshin, A., Hasekamp, O., Jones, D., Maksyutov, S., Marshall, J., Oda, T., O'Dell, C. W., Oshchepkov, S., Palmer, P. I., Peylin, P., Poussi, Z., Reum, F., Takagi, H., Yoshida, Y., and Zhuralev, R.: An intercomparison of inverse models for estimating sources and sinks of CO_2 using GOSAT measurements, J. Geophys. Res. Atmos., 120, 5253–5266, doi:10.1002/2014JD022962, 2015.

IPCC: Climate Change 2013: The Physical Science Basis, Working Group I Contribution to the Fifth Assessment Report of the Intergovernmental Report on Climate Change, http://www.ipcc.ch/report/ar5/wg1/ (last access: 21-February-2019), Cambridge University Press, 2013.

Jacobson, A. R., Schuldt, K. N., Miller, J. B., Oda, T., Tans, P., Andrews, A., Mund, J., Ott, L., Collatz, G. J., Aalto, T., Afshar, S., Aikin, K., Aoki, S., Apadula, F., Baier, B., Bergamaschi, P., Beyersdorf, A., Biraud, S. C., Bollenbacher, A., Bowling, D., Brailsford, G., Abshire, J. B., Chen, G., Chen, H., Chmura, L., Colomb, A., Conil, S., Cox, A., Cristofanelli, P., Cuevas, E., Curcoll, R., Sloop, C. D., Davis, K., Wekker, S. D., Delmotte, M., DiGangi, J. P., Dlugokencky, E., Ehleringer, J., Elkins, J. W., Emmenegger, L., Fischer, M. L., Forster, G., Frumau, A., Galkowski, M., Gatti, L. V., Gloor, E., Griffis, T., Hammer, S., Haszpra, L., Hatakka, J., Heliasz, M., Hensen, A., Hermanssen, O., Hintsa, E., Holst, J., Jaffe, D., Karion, A., Kawa, S. R., Keeling, R., Keronen, P., Kolari, P., Kominkova, K., Kort, E., Krummel, P., Kubistin, D., Labuschagne, C., Langenfelds, R., Laurent, O., Laurila, T., Lauvaux, T., Law, B., Lee, J., Lehner, I., Leuenberger, M., Levin, I., Levula, J., Lin, J., Lindauer, M., Loh, Z., Lopez, M., Lund Myhre, C., Machida, T., Mammarella, I., Manca, G., Manning, A., Manning, A., Marek, M. V., Marklund, P., Martin, M. Y., Matsueda, H., McKain, K., Meijer, H., Meinhardt, F., Miles, N., Miller, C. E., Mölder, M., Montzka, S., Moore, F., Morgui, J.-A., Morimoto, S., Munger, B., Necki, J., Newman, S., Nichol, S., Niwa, Y., O'Doherty, S., Ottosson-Löfvenius, M., Paplawsky, B., Peischl, J., Peltola, O., Pichon, J.-M., Piper, S., Plass-Dölmer, C., Ramonet, M., Reyes-Sanchez, E., Richardson, S., Riris, H., Ryerson, T., Saito, K., Sargent, M., Sasakawa, M., Sawa, Y., Say, D., Scheeren, B., Schmidt, M., Schmidt, A., Schumacher, M., Shepson, P., Shook, M., Stanley, K., Steinbacher, M., Stephens, B., Sweeney, C., Thoning, K., Torn, M., Turnbull, J., Tørseth, K., Bulk, P. V. D., Laan-Luijkx, I. T. V. D., Dinther, D. V., Vermeulen, A., Viner, B., Vitkova, G., Walker, S., Weyrauch, D., Wofsy, S., Worthy, D., Young, D., and Zimnoch, M.: CarbonTracker CT2019, DOI: 10.25925/39m3-6069, 2020.

Janssens-Maenhout, G., Pinty, B., Dowell, M., Zunker, H., Andersson, E., Balsamo, G., Bezy, J.-L., Brunhes, T., Boesch, H., Bojkov, B., Brunner, D., Buchwitz, M., Crisp, D., Ciais, P., Counet, P., Dee, D., Denier van der Gon, H., Dolman, H., Drinkwater, M., Dubovik, O., Engelen, R., Fehr, T., Fernandez, V., Heimann, M., Holmlund, K., Houweling, S., Husband, R., Juvyns, O., Kentarchos, A., Landgraf, J., Lang, R., Loescher, A., Marshall, J., Meijer, Y., Nakajima, M., Palmer, P. I., Peylin, P., Rayner, P., Scholze, M., Sierk, B., Tamminen, J., and Veefkind P.: Towards an operational anthropogenic CO_2 emissions monitoring and verification support capacity, Bulletin of the American Meteorological Society (BAMS), 10.1175/BAMS-D-19-0017.1, https://doi.org/10.1175/BAMS-D-19-0017.1, Published Online: 10 February 2020, 2020.

Kaminski, T., Scholze, M., Voßbeck, M., Knorr, W., Buchwitz, M, and Reuter, M.: Constraining a terrestrial biosphere model with remotely sensed atmospheric carbon dioxide, Remote Sensing of Environment 203, 109-124, 2017.

Kiel, M., O'Dell, C. W., Fisher, B., Eldering, A., Nassar, R., MacDonald, C. G., and Wennberg, P. O.: How bias correction goes wrong: measurement of XCO_2 affected by erroneous surface pressure estimates, Atmos. Meas. Tech., 12, 2241–2259, https://doi.org/10.5194/amt-12-2241-2019, 2019.

Kuhlmann, G., Broquet, G., Marshall, J., Clément, V., Löscher, A., Meijer, Y., and Brunner, D.: Detectability of CO_2 emission plumes of cities and power plants with the Copernicus Anthropogenic CO_2 Monitoring (CO2M) mission, Atmos. Meas. Tech., 12, 6695-6719, doi: 10.5194/amt-12-6695-2019, 2019.

Kulawik, S., Wunch, D., O'Dell, C., Frankenberg, C., Reuter, M., Oda, T., Chevallier, F., Sherlock, V., Buchwitz, M., Osterman, G., Miller, C. E., Wennberg, P. O., Griffith, D., Morino, I., Dubey, M. K., Deutscher, N. M., Notholt, J., Hase, F., Warneke, T., Sussmann, R., Robinson, J., Strong, K., Schneider, M., De Maziere, M., Shiomi, K., Feist, D. G., Iraci, L. T., Wolf, J.: Consistent evaluation of ACOS-GOSAT, BESD-SCIAMACHY, CarbonTracker, and MACC through comparisons to TCCON, Atmos. Meas. Tech., 9, 683-709, doi:10.5194/amt-9-683-2016, 2016.

Kuze, A., Suto, H., Shiomi, K., Kawakami, S., Tanaka, M., Ueda, Y., Deguchi, A., Yoshida, J., Yamamoto, Y., Kataoka, F., Taylor, T. E., and Buijs, H. L.: Update on GOSAT TANSO-FTS performance, operations, and data products after more than 6 years in space, Atmos. Meas. Tech., 9, 2445-2461, doi:10.5194/amt-9-2445-2016, 2016.

Labzovskii, L. D., Jeong, S.-J., and Parazoo, N. C.: Working towards confident spaceborne monitoring of carbon emissions from cities using Orbiting Carbon Observatory-2, Remote Sensing of Environment, 233, 111359, doi: 10.1016/j.rse.2019.111359, 2019.

Lauer, A., Eyring, V., Righi, M., Buchwitz, M., Defourny, P., Evaldsson, M., Friedlingstein, P., de Jeu, R., de Leeuw, G., Loew, A., Merchant, C. J., Müller, B., Popp, T., Reuter, M., Sandven, S., Senftleben, D., Stengel, M., Van Roozendael, M., Wenzel, S., and Willén, U.: Benchmarking CMIP5 models with a subset of ESA CCI Phase 2 data using the ESMValTool, Remote Sensing of Environment, 203, 9-39, http://dx.doi.org/10.1016/j.rse.2017.01.007, 2017.

Le Quéré, C., Andrew, R. M., Friedlingstein, P., Sitch, S., Pongratz, J., Manning, A. C., Korsbakken, J. I., Peters, G. P. Canadell, J. G., Jackson, R. B., Boden, T. A., Tans, P. P., Andrews, O. D., Arora, V. K., Bakker, D. D. E, Barbero, L., Becker, M., Betts, R. A., Bopp, L., Chevallier, F., Chini, L. P., Ciais, P., Cosca, C. E., Cross, J., Currie, K., Gasser, T., Harris, I., Hauck, J., Haverd, V., Houghton, R. A., Hunt, C. W., Hurtt, G., Ilyina, T., Jain, A. K., Kato, E., Kautz, M., Keeling, R. F., Goldewijk, K. K., Körtzinger, A., Landschützer, P., Lefèvre, N., Lenton, A., Lienert, S., Lima, I., Lombardozzi, D., Metzl, N., Millero, F., Monteiro, P. M. S., Munro, D. R., Nabel, J. E. M. S., Nakaoka, S., Nojiri, Y., Padín, X. A., Peregon, A., Pfeil, B., Pierrot, D., Poulter, B., Rehder, G., Reimer, J., Rödenbeck, C., Schwinger, J., Séférian, R., Skjelvan, I., Stocker, B. D., Tian, H., Tilbrook, B., van der Laan-Luijkx, I. T., van der Werf, G. R., van Heuven, S., Viovy,

N., Vuichard, N., Walker, A. P., Watson, A. J., Wiltshire, A. J., Zaehle, S., and Zhu, D.: Global Carbon Budget 2017, Earth System Science Data, 10, 405-448, DOI: 10.5194/essd-10-405-2018, 2018.

Le Quéré, C., Jackson, R. B., Jones, M. W., Smith, A. J. P., Abernethy, S., Andrew, R. M., De-Gol, A. J., Willis, D. R., Shan, Y., Canadell, J. G., Friedlingstein, P., Creutzig, G. and Peters, G. P.: Temporary reduction in daily global CO_2 emissions during the COVID-19 forced confinement. *Nat. Clim. Chang.* **10,** 647–653, https://doi.org/10.1038/s41558-020-0797-x (last access: 15-July-2020), 2020.

Liu, J., Bowman, K. W., Schimel, D. S., Parazoo, N. C., Jiang, Z., Lee, M., Bloom, A. A., Wunch, D., Frankenberg, C., Sun, Y., O'Dell, C. W., Gurney, K. R., Menemenlis, D., Gierach, M., Crisp, D., and Eldering, A.: Contrasting carbon cycle responses of the tropical continents to the 2015–2016 El Niño, Science, 358, eaam5690, pp. 7, 2017.

Liu, Z., Ciais, P., Deng, Z., Lei, R., Davis, S. J., Feng, S., Zheng, B., Cui, D., Dou, X., He, P., Zhu, B., Lu, C., Ke, P., Sun, T., Wang, Y., Yue, X., Wang, Y., Lei, Y., Zhou, H., Cai, Z., Wu, Y., Guo, R., Han, T., Xue, J., Boucher, O., Boucher, E., Chevallier, F., Wei, Y., Zhong, H., Kang, C., Zhang, N., Chen, B., Xi, F., Marie, F., Zhang, Q., Guan, D., Gong, P., Kammen, D. M., He, K., and Schellnhuber, H. J., https://arxiv.org/abs/2004.13614 (last access: 15-July-2020), in review, 2020.

Massart, S., Agusti-Panareda, A., Heymann, J., Buchwitz, M., Chevallier, F., Reuter, M., Hilker, M., Burrows, J. P., Deutscher, N. M., Feist, D. G., Hase, F., Sussmann, R., Desmet, F., Dubey, M. K., Griffith, D. W. T., Kivi, R., Petri, C., Schneider, M., and Velazco, V. A.: Ability of the 4-D-Var analysis of the GOSAT BESD XCO_2 retrievals to characterize atmospheric CO_2 at large and synoptic scales, Atmos. Chem. Phys., 16, 1653-1671, doi:10.5194/acp-16-1653-2016, 2016.

Matsunaga, T., and Maksyutov, S. (eds.): A Guidebook on the Use of Satellite Greenhouse Gases Observation Data to Evaluate and Improve Greenhouse Gas Emission Inventories, Satellite Observation Center, National Institute for Environmental Studies, Japan, 1st Edition, March 2018, pp. 137, https://www.nies.go.jp/soc/doc/GHG_Satellite_Guidebook_1st_12d.pdf (last access: 26-Aug-2020), 2018.

Miller, S. M., Michalak, A. M., Detmers, R. G., Hasekamp, O. P., Bruhwiler, L. M. P., and Schwietzke, S.: China's coal mine methane regulations have not curbed growing emissions, Nature Communications, volume 10, article number: 303, 2019.

Miller, S. M. and Michalak, A. M.: The impact of improved satellite retrievals on estimates of biospheric carbon balance, Atmos. Chem. Phys., 20, 323–331, https://doi.org/10.5194/acp-20-323-2020, 2020.

Nassar, R., Hill, T. G., McLinden, C. A., Wunch, D., Jones, D. B. A., and Crisp, D.: Quantifying CO_2 emissions from individual power plants from space. Geophysical Research Letters, 44, 10,045– 10,053. https://doi.org/10.1002/2017GL074702, 2017.

Noël, S., et al.: XCO_2 retrieval for GOSAT and GOSAT-2 based on the FOCAL algorithm, manuscript in preparation, 2020.

O'Dell, C. W., Connor, B., Bösch, H., O'Brien, D., Frankenberg, C., Castano, R., Christi, M., Eldering, D., Fisher, B., Gunson, M., McDuffie, J., Miller, C. E., Natraj, V., Oyafuso, F., Polonsky, I., Smyth, M., Taylor, T., Toon, G. C.,Wennberg, P. O., andWunch, D.: The ACOS CO_2 retrieval algorithm – Part 1: The ACOS CO_2 retrieval algorithm – Part 1: Description and validation against synthetic observations, Atmos. Meas. Tech., 5, 99–121, doi:10.5194/amt-5-99-2012, 2012.

O'Dell, C. W., Eldering, A., Wennberg, P. O., Crisp, D., Gunson, M. R., Fisher, B., Frankenberg, C., Kiel, M., Lindqvist, H., Mandrake, L., Merrelli, A., Natraj, V., Nelson, R. R., Osterman, G. B., Payne, V. H., Taylor, T. R., Wunch, D., Drouin, B. J., Oyafuso, F., Chang, A., McDuffie, J., Smyth, M., Baker, D. F., Basu, S., Chevallier, F., Crowell, S. M. R., Feng, L., Palmer, P. I., Dubey, M., García, O. E., 15 Griffith, D. W. T., Hase, F., Iraci, L. T., Kivi, R., Morino, I., Notholt, J., Ohyama, H., Petri, C., Roehl, C. M., Sha, M. K., Strong, K.,Sussmann, R., Te, Y., Uchino, O., and Velazco, V. A.: Improved Retrievals of Carbon Dioxide from the Orbiting Carbon Observatory-2 with the version 8 ACOS algorithm, Atmos. Meas. Tech., 11, 6539-6576, https://doi.org/10.5194/amt-11-6539-2018, 2018.

Osterman, G., O'Dell, C., Eldering A., Fisher, B., Crisp, D., Cheng, C., Frankenberg, C., Lambert, A., Gunson, M., Mandrake, L., Wunch, D.: Orbiting Carbon Observatory-2 & 3 (OCO-2 & OCO-3) Data Product User's Guide, Operational Level 2 Data Versions 10 and Lite File Version 10 and VEarly, Technical Report National Aeronautics and Space Administration, Jet Propulsion Laboratory, California Institute of Technology, Pasadena, California, USA, Version 1.0, Revision A, June 8, 2020, Data Release: 10 (OCO-2), VEarly (OCO-3), https://docserver.gesdisc.eosdis.nasa.gov/public/project/OCO/OCO2_OCO3_B10_DUG.pdf (last access: 17-Aug-2020), 2020.

Palmer, P. I., Feng, L., Baker, D., Chevallier, F., Bösch, H., and Somkuti, P.; Net carbon emissions from African biosphere dominate pan-tropical atmospheric CO_2 signal, Nature Communications 10, Article number: 3344, pp. 9, https://www.nature.com/articles/s41467-019-11097-w (last access: 15-July-2020), 2019.

Peters, W., Jacobson, A. R., Sweeney, C., Andrews, A. E., Conway, T. J., Masarie, K., Miller, J. B., Bruhwiler, L. M. P. Pétron, G., Hirsch, A. I., Worthy, D. E. J., van der Werf, G. R.,Randerson, J. T., Wennberg, P. O., Krol, M. C., and Tans, P. P.: An atmospheric perspective on North American carbon dioxide exchange: CarbonTracker, Proceedings of the National Academy of Sciences (PNAS) of the United States of America, 104,18925–18930,doi:10.1073/pnas.0708986104, 2007.

Pillai, D., M. Buchwitz, C. Gerbig, T. Koch, M. Reuter, H. Bovensmann, J. Marshall, J. P. Burrows, Tracking city CO_2 emissions from space using a high resolution inverse modeling approach: A case study for Berlin, Germany, Atmos. Chem. Phys., 16, 9591-9610, doi:10.5194/acp-16-9591-2016, 2016.

Pinty, B., Janssens-Maenhout, G., Dowell, M., Zunker, H., Brunhes, T., Ciais, P., Dee, D., Denier van der Gon, H., Dolman, H., Drinkwater, M., Engelen, R., Heimann, M., Holmlund, K., Husband, R., Kentarchos, A., Meijer, Y., Palmer, P., and Scholze, M.: An Operational Anthropogenic CO_2 Emissions Monitoring & Verification Support capacity - Baseline Requirements, Model Components and Functional Architecture, doi: 10.2760/39384, European Commission Joint Research

Centre, EUR 28736 EN, pp. 102, https://www.copernicus.eu/sites/default/files/2019-09/CO2_Red_Report_2017.pdf (last access: 26-Aug-2020), 2017.

Pinty, B., Ciais, P., Dee, D., Dolman, H., Dowell, M., Engelen, R., Holmlund, K., Janssens-Maenhout, G., Meijer, Y., Palmer, P., Scholze, M., Denier van der Gon, H., Heimann, M., Juvyns, O., Kentarchos, A., and Zunker, H.: An Operational Anthropogenic CO_2 Emissions Monitoring & Verification Support Capacity – Needs and high level requirements for in situ measurements, doi: 10.2760/182790, European Commission Joint Research Centre, EUR 29817 EN, pp. 77, https://www.copernicus.eu/sites/default/files/2019-09/CO2_Green_Report_2019.pdf (last access: 26-Aug-2020), 2019.

Reuter, M., Buchwitz, M., Schneising, O., Heymann, J., Bovensmann, H., and Burrows, J. P.: A method for improved SCIAMACHY CO_2 retrieval in the presence of optically thin clouds, Atmos. Meas. Tech., 3, 209-232, 2010.

Reuter, M., Bovensmann, H., Buchwitz, M., Burrows, J. P., Connor, B. J., Deutscher, N. M., Griffith, D. W. T., Heymann, J., Keppel-Aleks, G., Messerschmidt, J., Notholt, J., Petri, C., Robinson, J., Schneising, O., Sherlock, V., Velazco, V., Warneke, W., Wennberg, P. O., and Wunch, D.: Retrieval of atmospheric CO_2 with enhanced accuracy and precision from SCIAMACHY: Validation with FTS measurements and comparison with model results, J. Geophys. Res., 116, D04301, doi:10.1029/2010JD015047, 2011.

Reuter, M., Buchwitz, M., Schneising, O., Hase, F., Heymann, J., Guerlet, S., Cogan, A. J., Bovensmann, H., and Burrows, J. P.: A simple empirical model estimating atmospheric CO_2 background concentrations, Atmos. Meas. Tech., 5, 1349-1357, 2012.

Reuter, M., Boesch, H., Bovensmann, H., Bril, A., Buchwitz, M., Butz, A., Burrows, J. P., O'Dell, C. W., Guerlet, S., Hasekamp, O., Heymann, J. , Kikuchi, N., Oshchepkov, S., Parker, R., Pfeifer, S., Schneising, O., Yokota, T., and Yoshida, Y.: A joint effort to deliver satellite retrieved atmospheric CO_2 concentrations for surface flux inversions: the ensemble median algorithm EMMA, Atmos. Chem. Phys., 13, 1771-1780, 2013.

Reuter, M., Buchwitz, M., Hilker, M., Heymann, J., Schneising, O., Pillai, D., Bovensmann, H., Burrows, J. P., Bösch, H., Parker, R., Butz, A., Hasekamp, O., O'Dell, C. W., Yoshida, Y., Gerbig, C., Nehrkorn, T., Deutscher, N. M., Warneke, T., Notholt, J., Hase, F., Kivi, R., Sussmann, R., Machida, T., Matsueda, H., and Sawa, Y.: Satellite-inferred European carbon sink larger than expected, Atmos. Chem. Phys., 14, 13739-13753, 2014a.

Reuter, M., Buchwitz, M., Hilboll, A., Richter, A., Schneising, O., Hilker, M., Heymann, J., Bovensmann, H., and Burrows, J. P.: Decreasing emissions of NOx relative to CO_2 in East Asia inferred from satellite observations, Nature Geoscience, 28 Sept. 2014, doi:10.1038/ngeo2257, pp. 4, 2014b.

Reuter, M., Buchwitz, M., Schneising, O., Noël, S., Rozanov, V., Bovensmann, H., and Burrows, J. P.: A Fast Atmospheric Trace Gas Retrieval for Hyperspectral Instruments Approximating Multiple Scattering - Part 1: Radiative Transfer and a Potential OCO-2 XCO_2 Retrieval Setup, Remote Sens., 9, 1159, doi:10.3390/rs9111159, 2017a.

Reuter, M., Buchwitz, M., Schneising, O., Noël, S., Bovensmann, H., and Burrows, J. P.: A Fast Atmospheric Trace Gas Retrieval for Hyperspectral Instruments Approximating Multiple Scattering - Part 2: Application to XCO_2 Retrievals from OCO-2, Remote Sens., 9, 1102, doi:10.3390/rs9111102, 2017b.

Reuter, M., Buchwitz, M., Hilker, M., Heymann, J., Bovensmann, H., Burrows, J. P., Houweling, S., Liu, Y., Nassar, R., Chevallier, F., Ciais, P., Marshall, J., and Reichstein, M.: How much CO_2 is taken up by the European terrestrial biosphere? Bull. Amer. Meteor. Soc. doi:10.1175/BAMS-D-15-00310.1, 24 April 2017, 665-671, 2017c.

Reuter, M., Buchwitz, M., Schneising, O., Krautwurst, S., O'Dell, C. W., Richter, A., Bovensmann, H., and Burrows, J. P.: Towards monitoring localized CO_2 emissions from space: co-located regional CO_2 and NO_2 enhancements observed by the OCO-2 and S5P satellites, Atmos. Chem. Phys., https://www.atmos-chem-phys.net/19/9371/2019/, 19, 9371-9383, 2019.

Reuter, M., Buchwitz, M., Schneising, O., Noel, S., Bovensmann, H., Burrows, J. P., Boesch, H., Di Noia, A., Anand, J., Parker, R. J., Somkuti, P., Wu, L., Hasekamp, O. P., Aben, I., Kuze, A., Suto, H., Shiomi, K., Yoshida, Y., Morino, I., Crisp, D., O'Dell, C. W., Notholt, J., Petri, C., Warneke, T., Velazco, V. A., Deutscher, N. M., Griffith, D. W. T., Kivi, R., Pollard, D. F., Hase, F., Sussmann, R., Te, Y. V., Strong, K., Roche, S., Sha, M. K., De Maziere, M., Feist, D. G., Iraci, L. T., Roehl, C. M., Retscher, C., and Schepers, D.: Ensemble-based satellite-derived carbon dioxide and methane column-averaged dry-air mole fraction data sets (2003-2018) for carbon and climate applications, Atmos. Meas. Tech., 13, 789-819, https://doi.org/10.5194/amt-13-789-2020, 2020.

Rodgers, C. D., Inverse Methods for Atmospheric Sounding: Theory and Practice, World Scientific Publishing, 2000.

Schneising, O., Buchwitz, M., Burrows, J. P., Bovensmann, H., Reuter, M., Notholt, J., Macatangay, R., and Warneke, T.: Three years of greenhouse gas column-averaged dry air mole fractions retrieved from satellite – Part 1: Carbon dioxide, Atmos. Chem. Phys., 8, 3827–3853, https://doi.org/10.5194/acp-8-3827-2008, 2008.

Schneising, O., Heymann, J., Buchwitz, M., Reuter, M., Bovensmann, H., and Burrows, J. P.: Anthropogenic carbon dioxide source areas observed from space: assessment of regional enhancements and trends, Atmos. Chem. Phys., 13, 2445-2454, doi:10.5194/acp-13-2445-2013, 2013.

Schneising, O., Reuter, M., Buchwitz, M., Heymann, J., Bovensmann, H., and Burrows, J. P.: Terrestrial carbon sink observed from space: variation of growth rates and seasonal cycle amplitudes in response to interannual surface temperature variability, Atmos. Chem. Phys., 14, 133-141, 2014.

Schwandner, F. M., Gunson, M. R., Miller, C. E., Carn, S. A., Eldering, A., Krings, T., Verhulst, K. R., Schimel, D. S., Nguyen, H. M., Crisp, D., O'Dell, C. W., Osterman, G. B., Iraci, L. T., and Podolske, J. R.: Spaceborne detection of localized carbon dioxide sources, Science, 358, eaam5782, doi: 10.1126/science.aam5782, 2017.

Sussmann, R., and Rettinger, M.: Can We Measure a COVID-19-Related Slowdown in Atmospheric CO_2 Growth? Sensitivity of Total Carbon Column Observations, Remote Sens., 12, 2387, https://www.mdpi.com/2072-4292/12/15/2387 (last access: 5-Oct-2020), 2020.

Veefkind, J. P., Aben, I., McMullan, K., Förster, H., De Vries, J., Otter, G., Claas, J., Eskes, H. J., De Haan, J. F., Kleipool, Q., Van Weele, M., Hasekamp, O., Hoogeveen, R., Landgraf, J., Snel, R., Tol, P.,Ingmann, P., Voors, R., Kruizinga, B., Vink, R., Visser, H., and Levelt, P. F.: TROPOMI on the ESA Sentinel-5 Precursor: A GMES mission for global observations of the atmospheric composition for climate, air quality and ozone layer applications. Rem. Sens. Environment, 120:70–83, 2012.

Velazco, V. A., M. Buchwitz, H. Bovensmann, M. Reuter, O. Schneising, J. Heymann, T. Krings, K. Gerilowski, and J. P. Burrows, Towards space based verification of CO_2 emissions from strong localized sources: fossil fuel power plant emissions as seen by a CarbonSat constellation, Atmos. Meas. Tech., 4, 2809-2822, 2011.

Wu, L., Hasekamp, O., Hu, H., Landgraf, J., Butz, A., aan de Brugh, J., Aben, I., Pollard, D. F., Griffith, D. W. T., Feist, D. G., Koshelev, D., Hase, F., Toon, G. C., Ohyama, H., Morino, I., Notholt, J., Shiomi, K., Iraci, L., Schneider, M., de Mazière, M., Sussmann, R., Kivi, R., Warneke, T., Goo, T.-Y., and Té, Y.: Carbon dioxide retrieval from OCO-2 satellite observations using the RemoTeC algorithm and validation with TCCON measurements, Atmos. Meas. Tech., 11, 3111–3130, https://doi.org/10.5194/amt-11-3111-2018, 2018.

Wu, L., Aben, I., and Hasekamp, O. P.: Product User Guide and Specification (PUGS) – ANNEX B for products CO2_GOS_SRFP, CH4_GOS_SRFP (v2.3.8, 2009-2018), 29-Nov-2019, pp. 26, http://wdc.dlr.de/C3S_312b_Lot2/Documentation/GHG/PUGS/C3S_D312b_Lot2.3.2.3-v1.0_PUGS-GHG_ANNEX-B_v3.1.pdf (last access: 17-Aug-2020), 2019.

Wu, D., Lin, J., Oda, T., and Kort, E.: Space-based quantification of per capita CO_2 emissions from cities, Environ. Res. Lett. 15, pp. 9, https://iopscience.iop.org/article/10.1088/1748-9326/ab68eb/pdf (last access: 15-July-2020), 2020.

Wunch, D., Toon, G.C.,Wennberg, P.O.,Wofsy, S.C., Stephens, B.B., Fischer, M.L., Uchino, O., Abshire, J.B., Bernath, P., Biraud, S.C., Blavier, J.-F.L., Boone, C., Bowman, K.P., Browell, E.V., Campos, T., Connor, B.J., Daube, B.C., Deutscher, N.M., Diao, M., Elkins, J.W., Gerbig, C., Gottlieb, E., Griffith, D.W.T., Hurst, D.F., Jimenez, R., Keppel-Aleks, G., Kort, E.A., Macatangay, R., Machida, T., Matsueda, H., Moore, F., Morino, I., Park, S., Robinson, J., Roehl, C.M., Sawa, Y., Sherlock, V., Sweeney, C., Tanaka, T., Zondlo, M.A.: Calibration of the total carbon column observing network using aircraft profile data. Atmos. Meas. Tech. 3:1351–1362. http://dx.doi.org/10.5194/amt-3-1351-2010, 2010.

Wunch, D., Toon, G. C., Blavier, J.-F. L., Washenfelder, R. A., Notholt, J., Connor, B. J., Griffith, D. W. T., Sherlock, V., and Wennberg, P. O.: The Total Carbon Column Observing Network. Phil. Trans. R. Soc. A, 369, 2087–2112, doi:10.1098/rsta.2010.0240, 2011.

745 Wunch, D., Wennberg, P. O., Osterman, G., Fisher, B., Naylor, B., Roehl, C. M., O'Dell, C., Mandrake, L., Viatte, C., Kiel, M., Griffith, D. W. T., Deutscher, N. M., Velazco, V. A., Notholt, J., Warneke, T., Petri, C., De Maziere, M., Sha, M. K., Sussmann, R., Rettinger, M., Pollard, D., Robinson, J., Morino, I., Uchino, O., Hase, F., Blumenstock, T., Feist, D. G., Arnold, S. G., Strong, K., Mendonca, J., Kivi, R., Heikkinen, P., Iraci, L., Podolske, J., Hillyard, P. W., Kawakami, S., Dubey, M. K., Parker, H. A., Sepulveda, E., García, O. E., Te, Y., Jeseck, P., Gunson, M. R., Crisp, D., and Eldering, A.:
750 Comparisons of the Orbiting Carbon Observatory-2 (OCO-2) XCO_2 measurements with TCCON, Atmos. Meas. Tech., 10, 2209-2238, do:10.5194/amt-10-2209-2017, 2017.

Wunch, D., Mendonca, J., Colebatch, O., Allen, N. T., Blavier, J.-F., Roche, S., Hedelius, J., Neufeld, G., Springett, S., Worthy, D., Kessler, R., and Strong, K.: TCCON data from East Trout Lake, SK (CA), Release GGG2014.R1. TCCON data archive, hosted by CaltechDATA, https://doi.org/10.14291/tccon.ggg2014.easttroutlake01.R1, 2018.

755 Ye, X., Lauvaux, T., Kort, E. A., Oda, T., Feng, S., Lin, J. C., Yang, E. G., and Wu, D.: Constraining fossil fuel CO_2 emissions from urban area using OCO-2 observations of total column CO_2, Journal of Geophysical Research: Atmospheres, 125, e2019JD030528. https://doi.org/10.1029/2019JD030528, 2020.

Yin, Y., Ciais, P., Chevallier, F., Li, W., Bastos, A., Piao, S., Wang, T., and Liu, H.: Changes in the response of the Northern Hemisphere carbon uptake to temperature over the last three decades. Geophysical Research Letters, 45, 4371– 4380,
760 https://doi.org/10.1029/2018GL077316, 2018.

Yoshida, Y., Kikuchi, N., Morino, I., Uchino, O., Oshchepkov, S., Bril, A., Saeki, T., Schutgens, N., Toon, G. C., Wunch, D., Roehl, C. M., Wennberg, P. O., Griffith, D. W. T, Deutscher, N. M., Warneke, T., Notholt, J., Robinson, J., Sherlock, V., Connor, B., Rettinger, M., Sussmann, R., Ahonen, P., Heikkinen, P., Kyrö, E., Mendonca, J., Strong, K., Hase, F., Dohe, S., and Yokota, T.: Improvement of the retrieval algorithm for GOSAT SWIR XCO_2 and XCH_4 and their validation using
765 TCCON data, Atmos. Meas. Tech., 6, 1533–1547, doi:10.5194/amt-6-1533-2013, 2013.

Zhang, R., Zhang, Y., Lin, H., Feng, X., Fu, T.-M., and Wang, Y.: NOx Emission Reduction and Recovery during

COVID-19 in East China, Atmosphere, 11, 433, pp. 15, doi:10.3390/atmos11040433, 2020.

Zheng, B., Chevallier, F., Ciais, P., Broquet, G., Wang, Y., Lian, J., and Zhao, Y.: Observing carbon dioxide emissions over China's cities with the Orbiting Carbon Observatory-2, Atmos. Chem. Phys. Discuss., https://doi.org/10.5194/acp-2020-123
770 ((last access: 15-July-2020), in review, 2020a.

Zheng, B., Geng, G., Ciais, P., Davis, S. J., Martin, R. V., Meng, J., Wu, N., Chevallier, F., Broquet, G., Boersma, F., van der A., R., Lin, J., Guan, D., Lei, Y., He, Kebin, and Zhang, Q.: Satellite-based estimates of decline and rebound in China's CO_2 emissions during COVID-19 pandemic, https://arxiv.org/ftp/arxiv/papers/2006/2006.08196.pdf (last access: 15-July-2020), pp. 46, in review, 2020b.

775

https://doi.org/10.5194/amt-2020-386
Preprint. Discussion started: 8 October 2020

Atmospheric Measurement Techniques Discussions

Tables:

Table 1. Overview of the satellite XCO_2 Level 2 (L2) input data products. (#) These products are available via the Copernicus Climate Data Store (CDS, https://cds.climate.copernicus.eu/cdsapp#!/dataset/satellite-carbon-dioxide?tab=overview (last access: 23-September-2020)) until end of 2019. Year 2020 data will be made available via the CDS in 2021 but are also available from the authors on request.

Satellite	Algorithm	Product version	Product ID	References	Data provider and data access information
OCO-2	ACOS	v10r	CO2_OC2_ACOS	O'Dell et al., 2018; Kiel et al., 2019; Osterman et al., 2020	Product "OCO2_L2_Lite_FP 10r" obtained from NASA's Earthdata GES DISC website: https://disc.gsfc.nasa.gov/datasets?keywords=OCO-2%20v10r&page=1 (last access: 15-Aug-2020)
GOSAT	UoL-FP	v7.3	CO2_GOS_OCFP	Cogan et al., 2012; Boesch et al., 2019	Generated by authors (#)
GOSAT	RemoTeC	v2.3.8	CO2_GOS_SRFP	Butz et al., 2011; Wu et al., 2019	Generated by authors (#)
GOSAT	FOCAL	v1.0	CO2_GOS_FOCA	Noël et al., 2020	Generated by authors and available on request

https://doi.org/10.5194/amt-2020-386
Preprint. Discussion started: 8 October 2020

Atmospheric Measurement Techniques Discussions

Table 2. Overview of the CarbonTracker CT2019 data set. For this study we used data from the period January 2015 to December 2018.

Model / Version	Details	Reference	Access
CarbonTracker CT2019	Atmospheric CO_2 molefraction profiles (spatio-temporal sampling: 3°x2°, 3-hourly) and CO_2 fluxes (spatio-temporal sampling: 1°x1°, 3-hourly)	Jacobson et al., 2020 DOI: http://dx.doi.org/10.25925/39m3-6069 (last access: 22-July-2020)	CarbonTracker CT2019, http://carbontracker.noaa.gov (last access: 22-July-2020)

Table 3. Corner coordinates of the East China target region as analysed in this study.

Region ID	Latitude range [deg North]	Lontitude range [deg East]
East China	28 – 44	102 – 126

https://doi.org/10.5194/amt-2020-386
Preprint. Discussion started: 8 October 2020

Atmospheric Measurement Techniques Discussions

795

Table 4. Numerical values of the ensemble-based ΔXCO_2^{FF} results as shown in Fig. 13. Listed are the median values and corresponding 1-sigma uncertainties (in brackets). The dimensionless values listed here represent the relative ΔXCO_2^{FF} change for January-May 2020 relative to October-December 2019 and previous years. The listed data refer to the difference relative to October to December 2019, i.e., the corresponding offset (October to December 2019 mean) has been subtracted.

800

Month Product ID	October 2019	November 2019	December 2019	January 2020	February 2020	March 2020	April 2020	May 2020
CO2_OC2_ACOS	0.000 (0.023)	0.005 (0.032)	-0.005 (0.018)	0.015 (0.029)	-0.008 (0.020)	-0.007 (0.016)	-0.023 (0.017)	-0.016 (0.028)
CO2_GOS_OCFP	-0.084 (0.077)	0.025 (0.074)	0.058 (0.053)	-0.133 (0.035)	-0.056 (0.051)	-0.151 (0.087)	-0.242 (0.031)	-0.110 (0.160)
CO2_GOS_SRFP	-0.067 (0.039)	0.130 (0.045)	-0.063 (0.049)	0.043 (0.091)	-0.064 (0.061)	0.024 (0.093)	-0.106 (0.046)	0.010 (0.082)
CO2_GOS_FOCA	-0.048 (0.049)	0.052 (0.062)	-0.004 (0.043)	-0.041 (0.042)	-0.016 (0.104)	-0.189 (0.057)	-0.040 (0.070)	-0.110 (0.063)
Ensemble	-0.050 (0.036)	0.053 (0.055)	-0.004 (0.049)	-0.029 (0.078)	-0.036 (0.028)	-0.081 (0.105)	-0.103 (0.099)	-0.057 (0.063)

805

https://doi.org/10.5194/amt-2020-386
Preprint. Discussion started: 8 October 2020

Atmospheric Measurement Techniques Discussions

Figures:

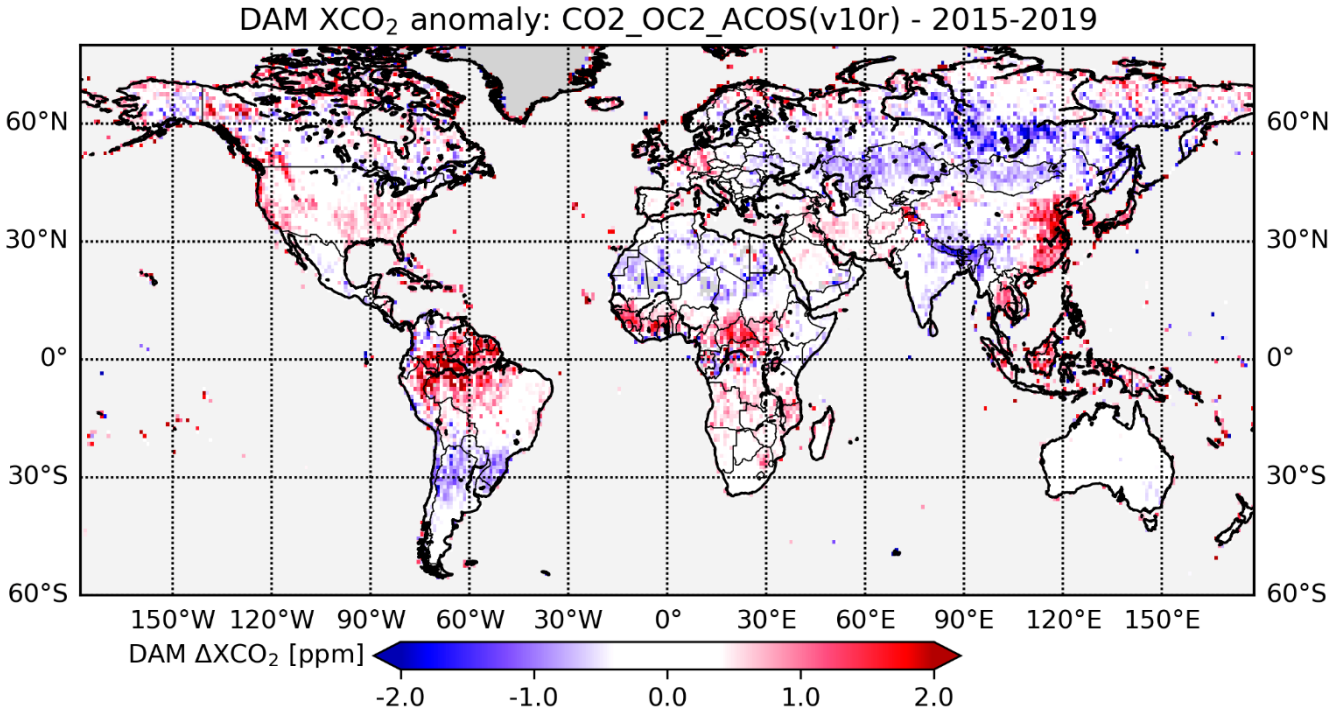

Figure 1: DAM XCO_2 anomaly map at 1º x 1º resolution generated from OCO-2 Level 2 XCO_2 (v10r, land) for 2015 to 2019.

https://doi.org/10.5194/amt-2020-386
Preprint. Discussion started: 8 October 2020

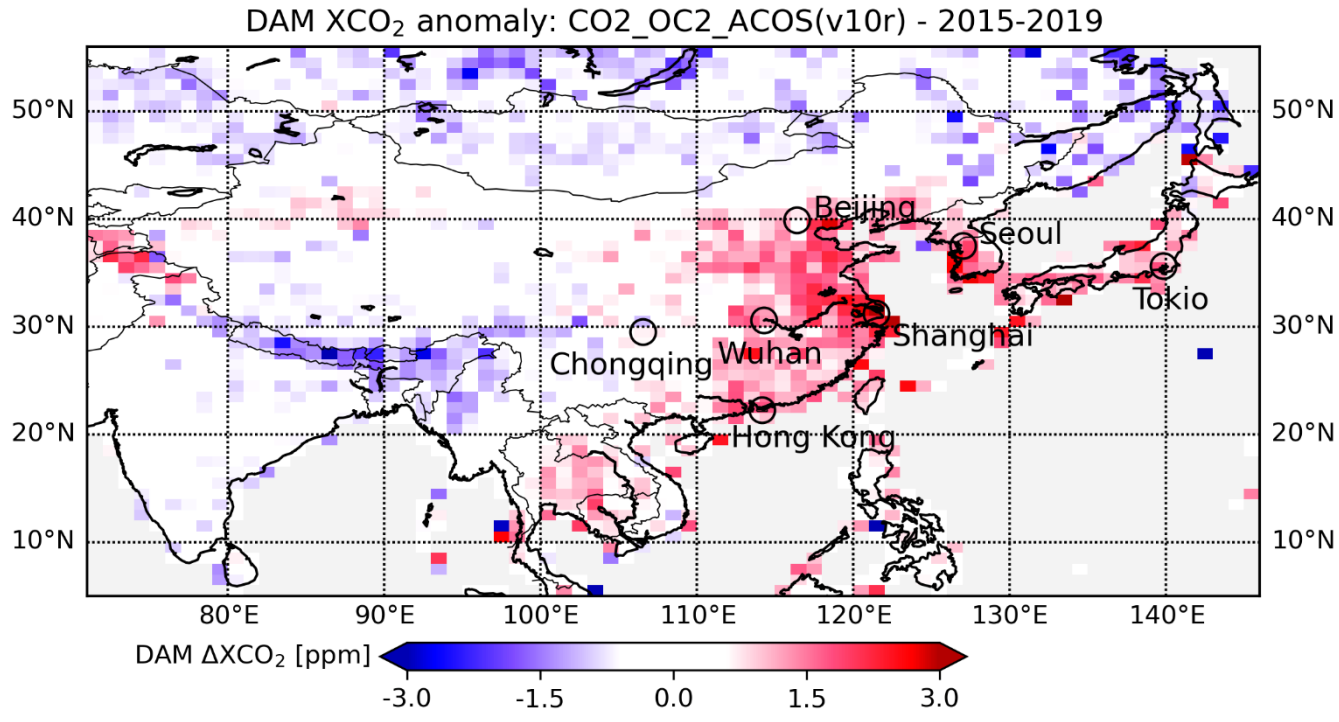

Figure 2: As Fig. 1 but for China and surrounding areas.

820

https://doi.org/10.5194/amt-2020-386
Preprint. Discussion started: 8 October 2020

Atmospheric Measurement Techniques Discussions

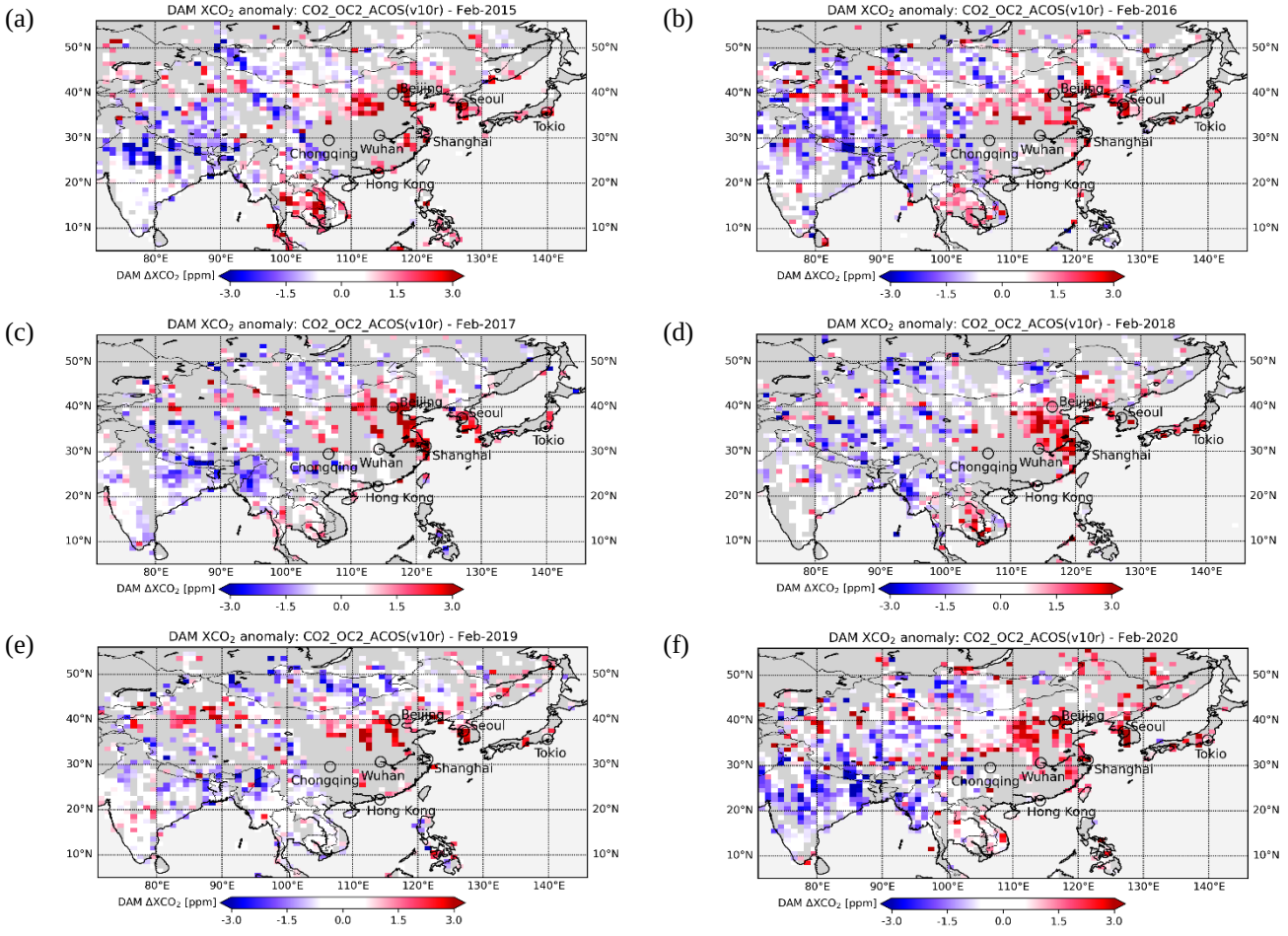

Figure 3: As Fig. 2 but for (a) February 2015 to (f) February 2020.

825

https://doi.org/10.5194/amt-2020-386
Preprint. Discussion started: 8 October 2020

Atmospheric Measurement Techniques Discussions

(a)

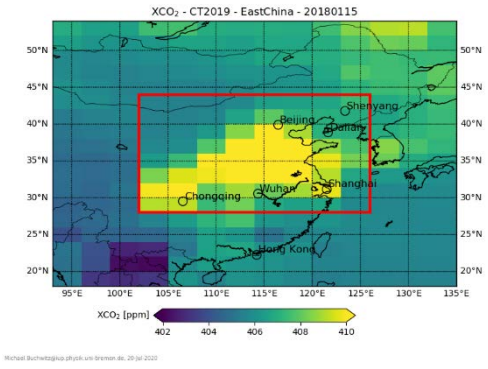

(b)

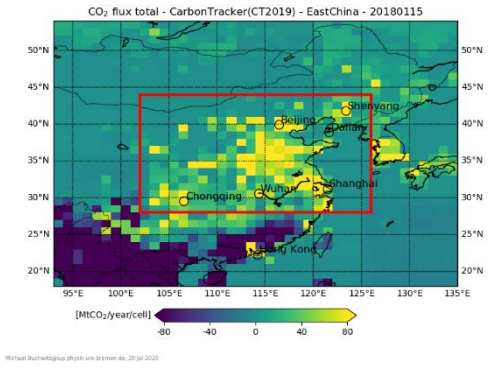

(c)

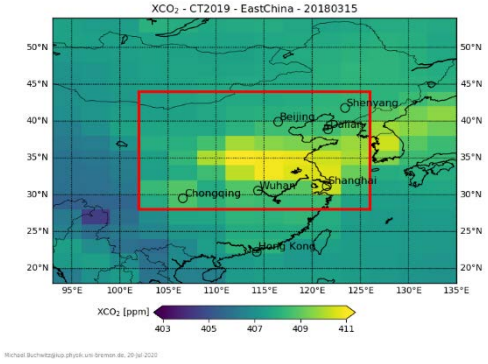

(d)

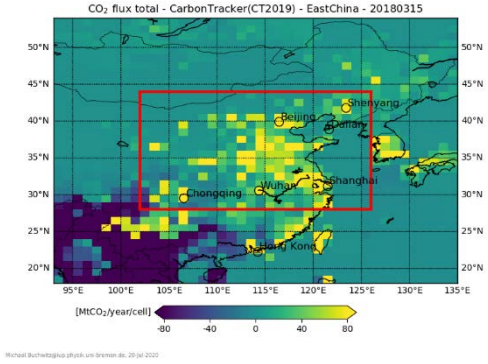

(e)

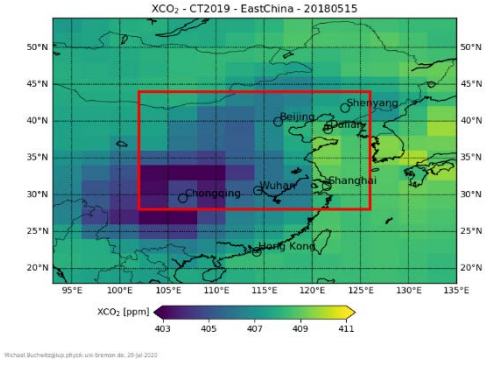

(f)

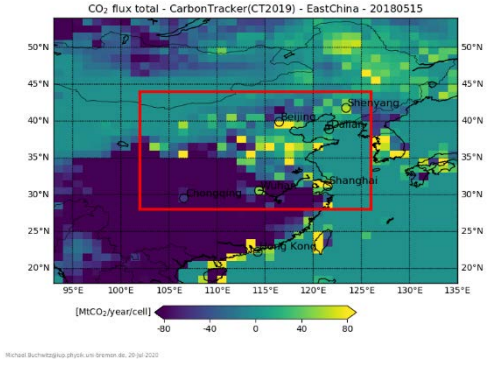

Figure 4: Left: CT2019 XCO_2 (left, in ppm) and corresponding CO_2 surface fluxes (right, in $MtCO_2$/year/cell) for 15-Jan-2018 (first row), 15-Mar-2018 (middle) and 15-May-2018 (bottom). The red rectangle encloses the East China target region as defined for this study.

https://doi.org/10.5194/amt-2020-386
Preprint. Discussion started: 8 October 2020

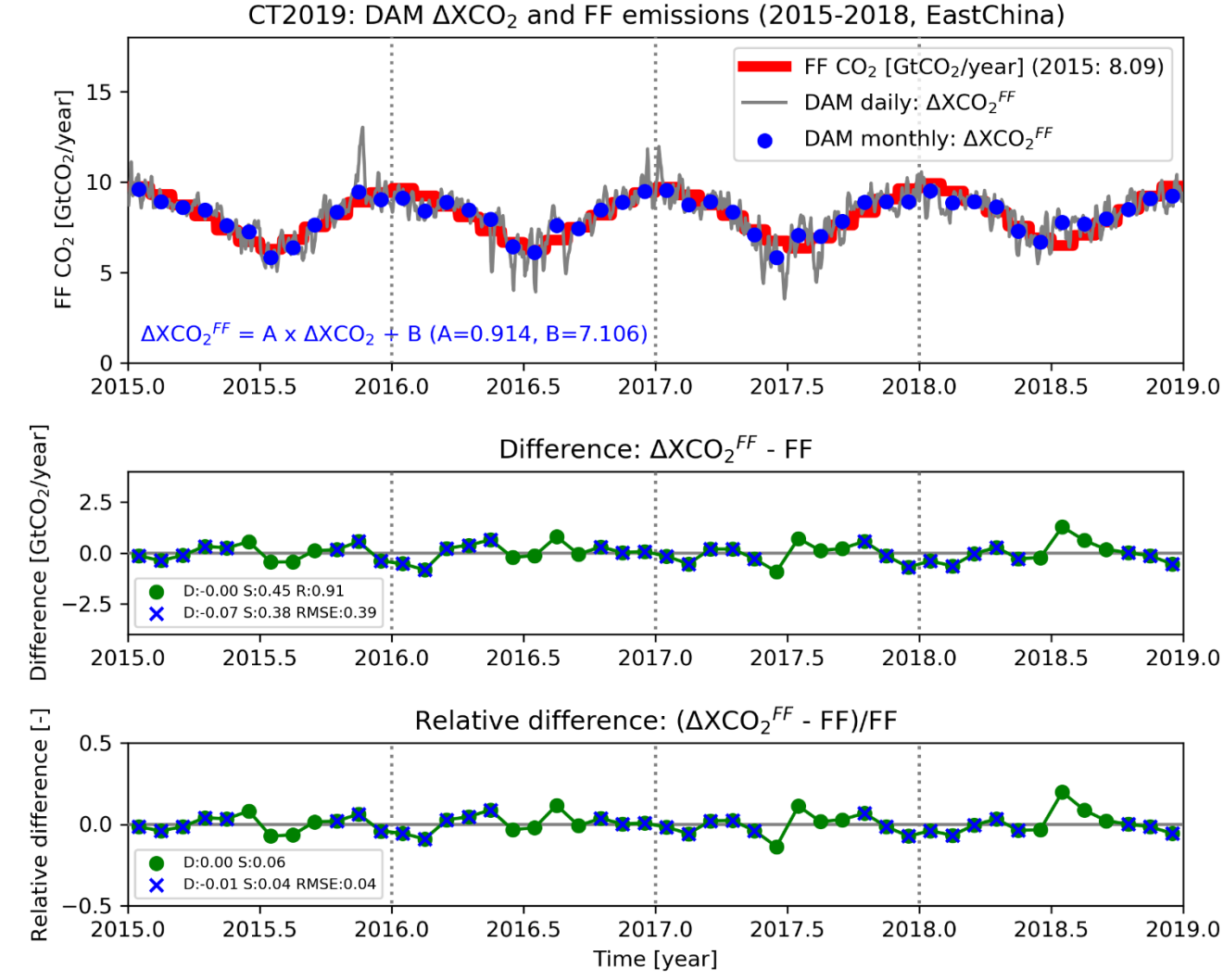

Michael.Buchwitz@iup.physik.uni-bremen.de, 20-July-2020

Figure 5: Results obtained by applying the DAM method to CT2019 XCO_2. Top panel: The thick red line shows the CT2019 fossil fuel (FF) monthly CO_2 emissions in $GtCO_2$/year for target region East China. The thin grey line shows daily ΔXCO_2^{FF} and the blue dots show monthly ΔXCO_2^{FF} (see main text for a detailed explanation). Middle panel: Absolute difference between monthly ΔXCO_2^{FF} and the CT2019 FF target region emissions. Listed is the mean difference D, the standard deviation of the difference S, the linear correlation coefficient R and the root-mean-square error (RMSE). All quantities (except R) are listed for all months (green dots) and separately for the months October to May (blue crosses). Bottom panel: the same as the middle panel but for the relative differences (as fraction, not percent, see panel title) instead of the absolute differences.

https://doi.org/10.5194/amt-2020-386
Preprint. Discussion started: 8 October 2020

Atmospheric Measurement Techniques Discussions

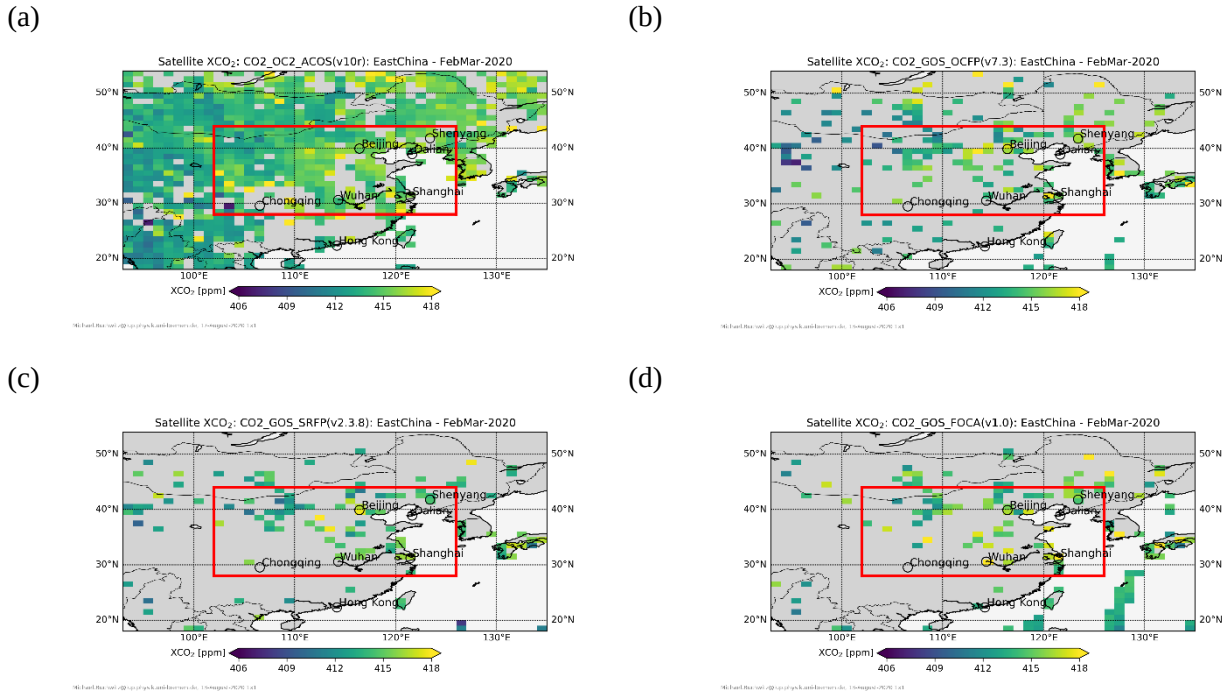

845

Figure 6: (a): OCO-2 XCO_2 (version 10r, product ID CO2_OC2_ACOS) over land at 1ºx1º resolution for February-March 2020. The red rectangle encloses the investigated East China target region. (b)-(d) as (a) but for products CO2_GOS_OCFP (b), CO2_GOS_SRFP (c), and CO2_GOS_FOCA (d) (see Tab. 1 for details).

850

https://doi.org/10.5194/amt-2020-386
Preprint. Discussion started: 8 October 2020

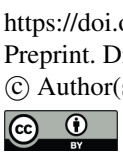

Atmospheric Measurement Techniques Discussions

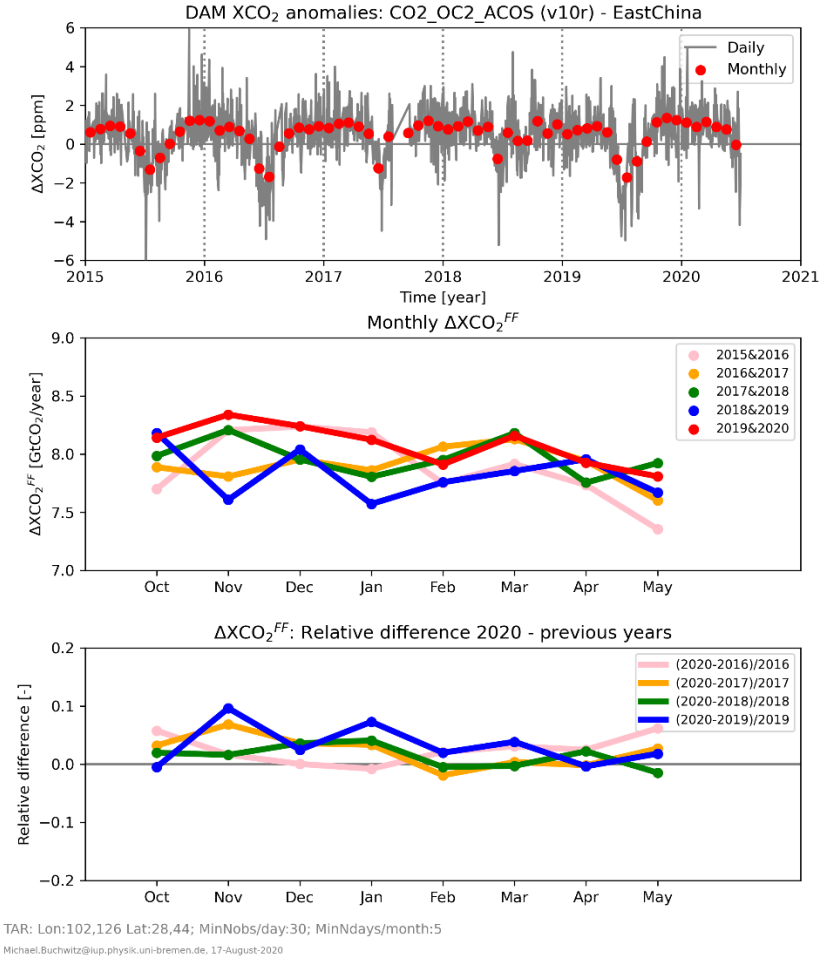

Figure 7: DAM analysis of the OCO-2 ACOS version 10r XCO_2 product (CO2_OC2_ACOS) for the region East China from January 2015 to May 2020. Top: The thin grey line shows the daily DAM XCO_2 anomalies, i.e., daily DAM ΔXCO_2. The red dots are the corresponding monthly values. Middle: Monthly ΔXCO_2^{FF}. The red dots (and lines) refer to the time period October 2019 – May 2020, the blue dots to period October 2018 – May 2019, the green dots to period October 2017 – May 2018, etc. (see annotation). Bottom panel: the same as the middle panel but for relative differences of the monthly values: Blue dots: relative difference of the values of the red dots shown in the middle panel (ending May 2020) and the blue dots shown in the middle panel (ending May 2019) denoted in the annotation as "(2020-2019)/2019". Also shown are the relative differences for 2020 and 2018 (green), 2020 and 2017 (orange) and 2020 and 2016 (pink). The following parameters have been used to generate this figure: Minimum number of observations/day: 30, minimum number of days/month: 5.

https://doi.org/10.5194/amt-2020-386
Preprint. Discussion started: 8 October 2020

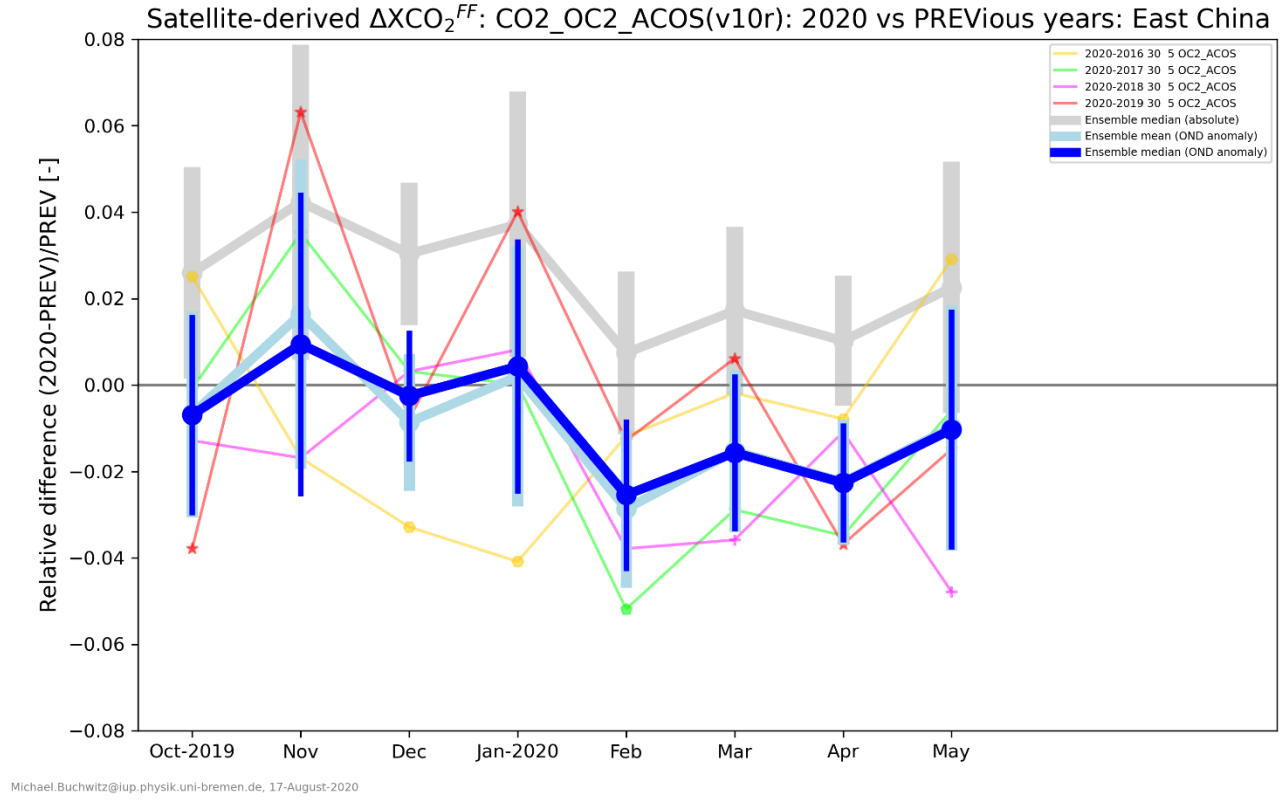

Figure 8: Product CO2_OC2_ACOS ΔXCO_2^{FF} differences as shown in the bottom panel of Fig. 7 but including the corresponding median, mean and scatter. The relative differences as shown in the bottom panel of Fig. 7 are shown here via small symbols with thin connecting lines (using different colours for different years, see annotation) and with an offset subtracted, which corresponds to the October to December (OND) 2019 mean value, i.e., the data are shown here as anomaly relative to OND 2019 ("OND anomaly"). The corresponding median and standard deviation is shown in royal blue (the corresponding mean and standard deviation is show in light blue). The median of the original data (no offset subtracted) is shown as thick grey dots and lines, i.e., the offset is the difference between the royal blue and the grey lines. The following parameters have been used to generate this figure (see also annotation): Minimum number of observations/day: 30; minimum number of days/month: 5.

https://doi.org/10.5194/amt-2020-386
Preprint. Discussion started: 8 October 2020

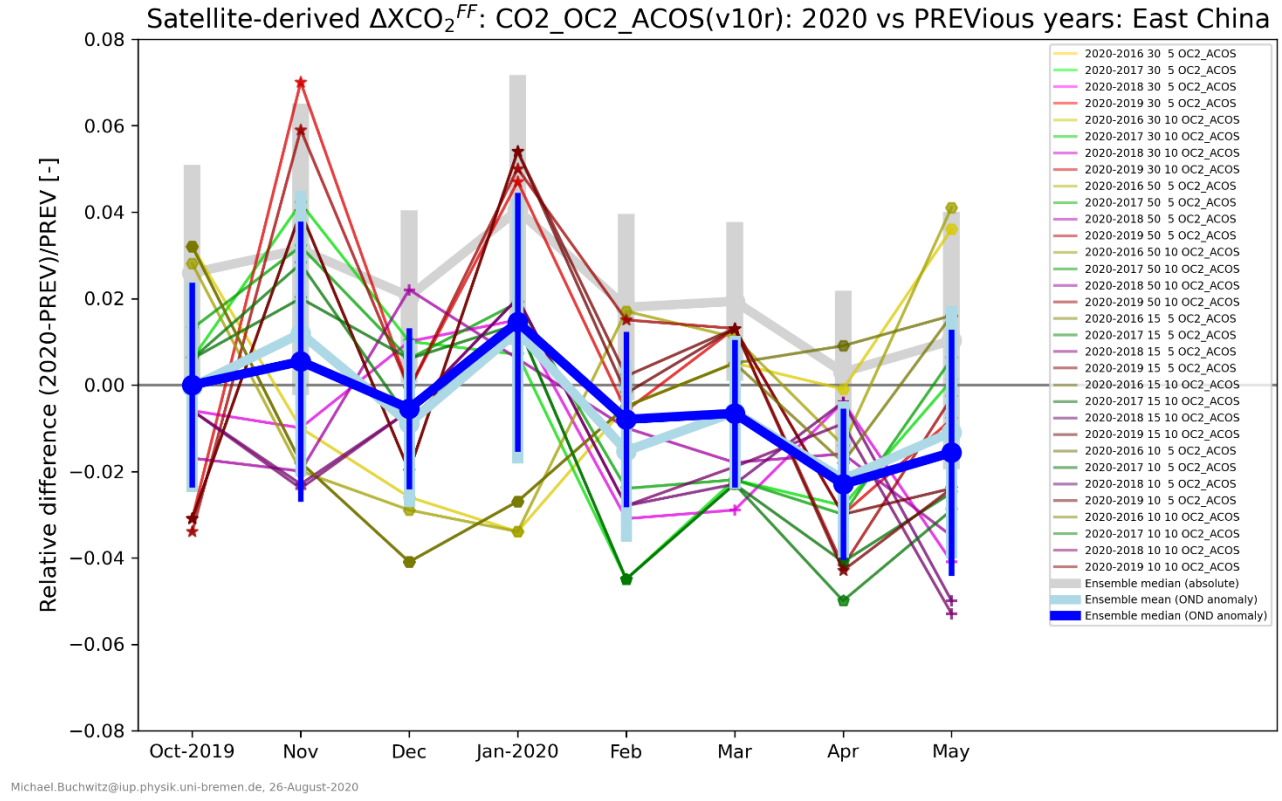

Figure 9: The same as Fig. 8 but with additional combinations of minimum number of observations/day (30 as in Fig. 8 and in addition: 50, 15 and 10) and minimum number of days/month (5 as in Fig. 8 and in addition 10) (see annotation).

https://doi.org/10.5194/amt-2020-386
Preprint. Discussion started: 8 October 2020

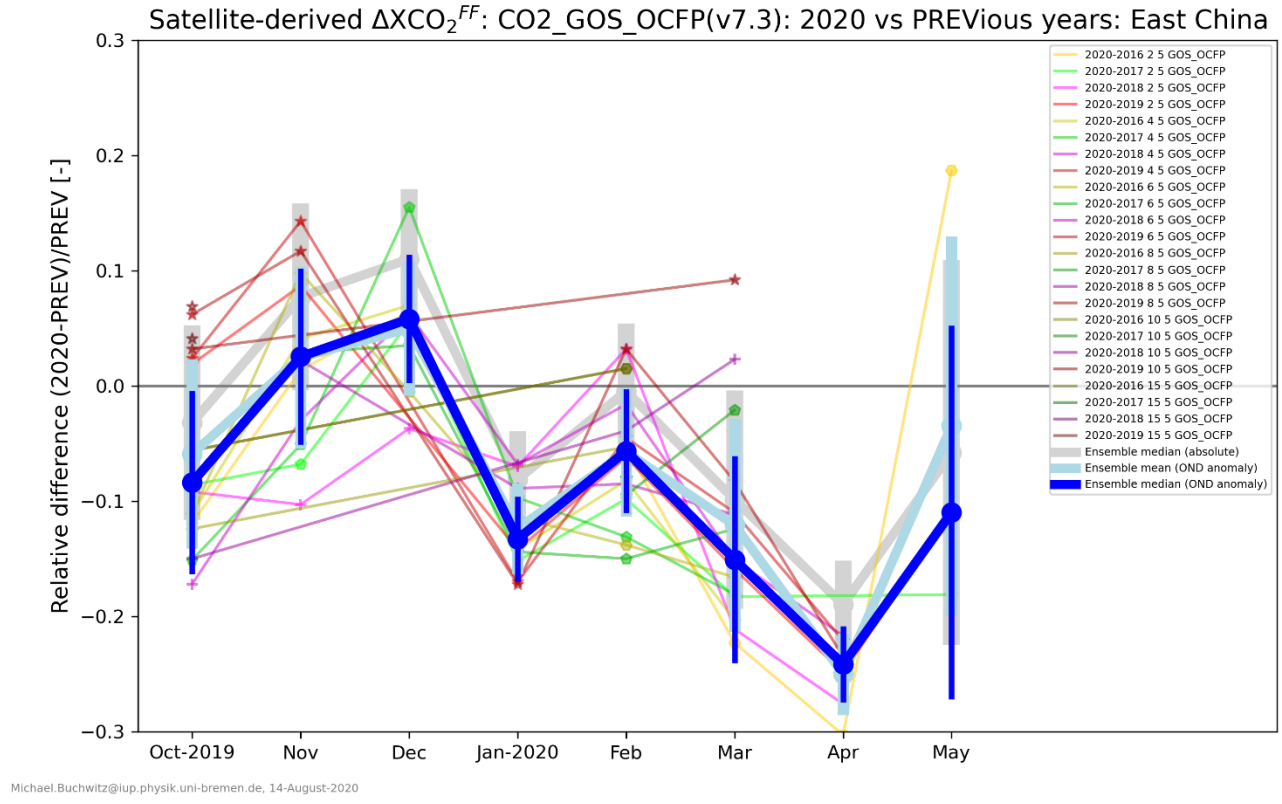

Figure 10: The same as Figs. 9 but for the product CO2_GOS_OCFP. Results are shown for several values of the required minimum number of observations/day: 2, 4, 6, 8, 10 and 15. The required minimum number of days/month is 5.

https://doi.org/10.5194/amt-2020-386
Preprint. Discussion started: 8 October 2020

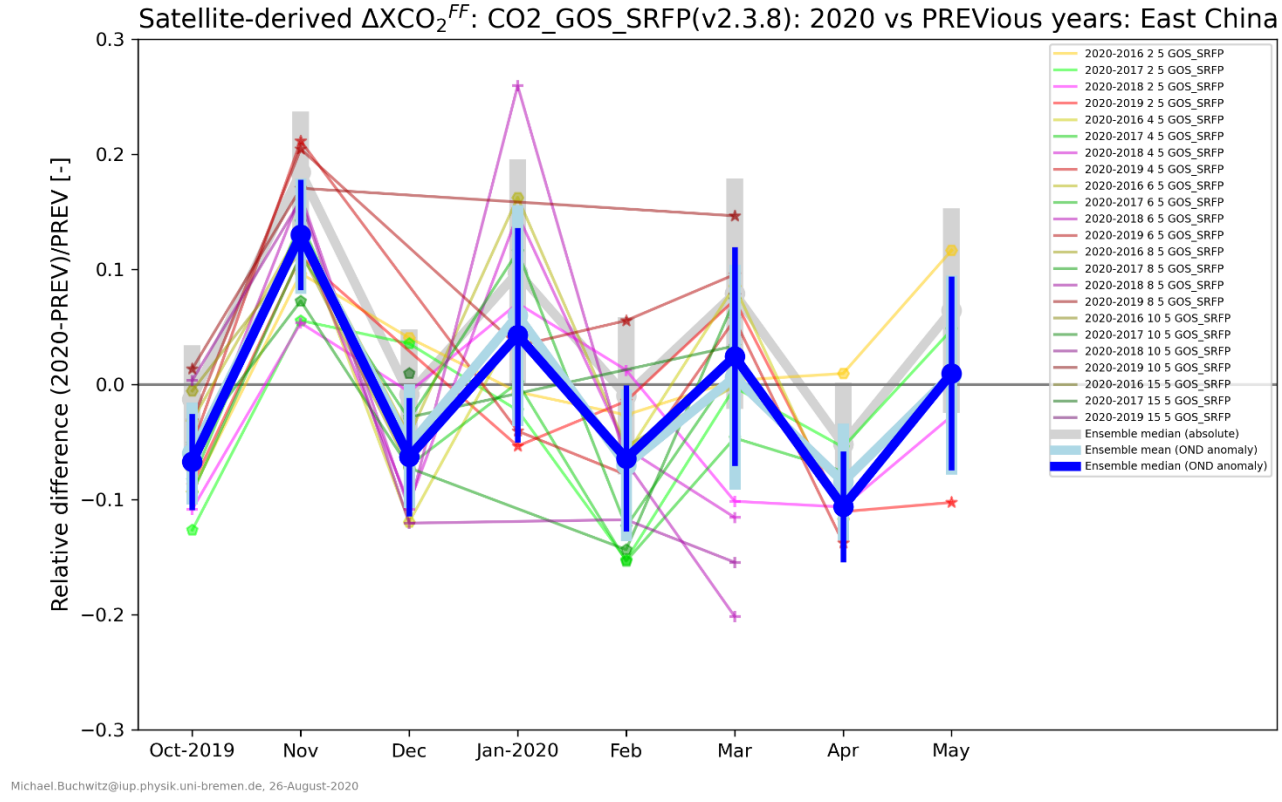

Figure 11: The same as Fig. 10 but for the product CO2_GOS_SRFP.

https://doi.org/10.5194/amt-2020-386
Preprint. Discussion started: 8 October 2020

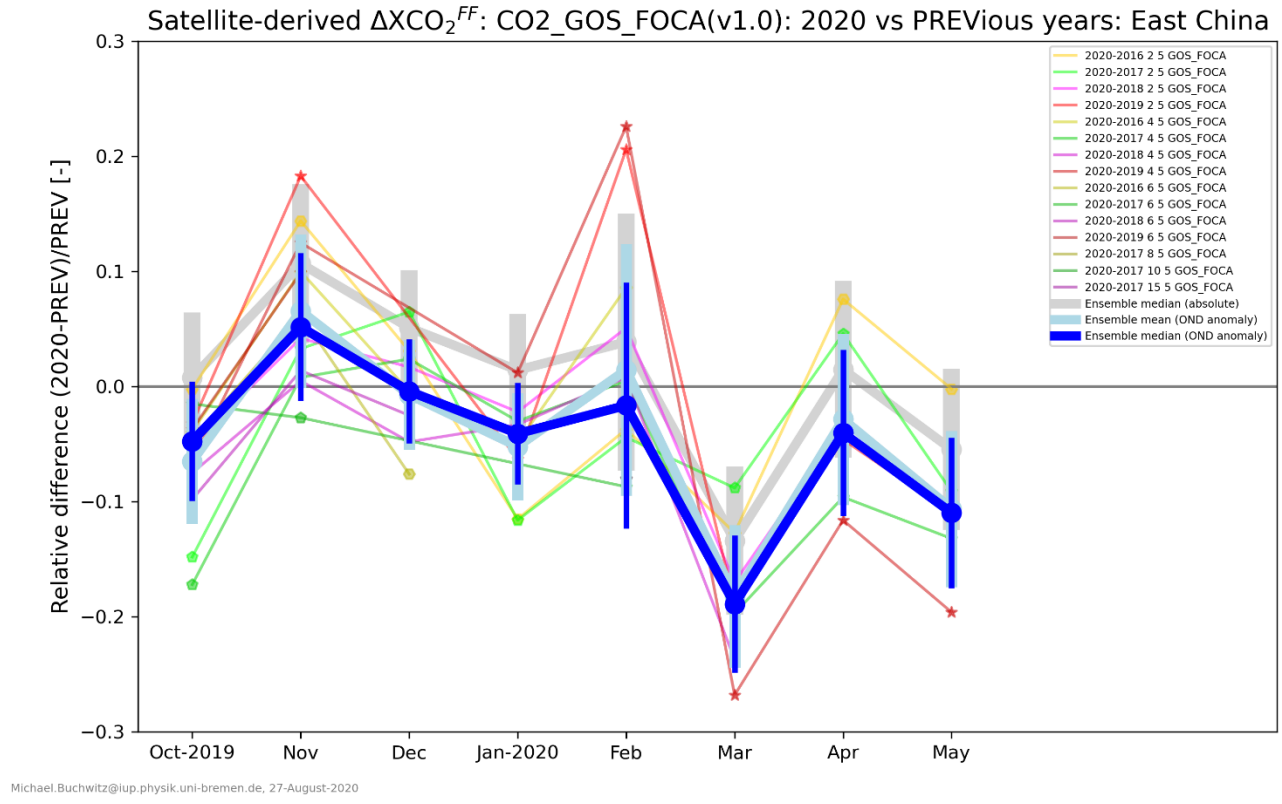

900

Figure 12: The same as Fig. 10 but for the product CO2_GOS_FOCA.

https://doi.org/10.5194/amt-2020-386
Preprint. Discussion started: 8 October 2020

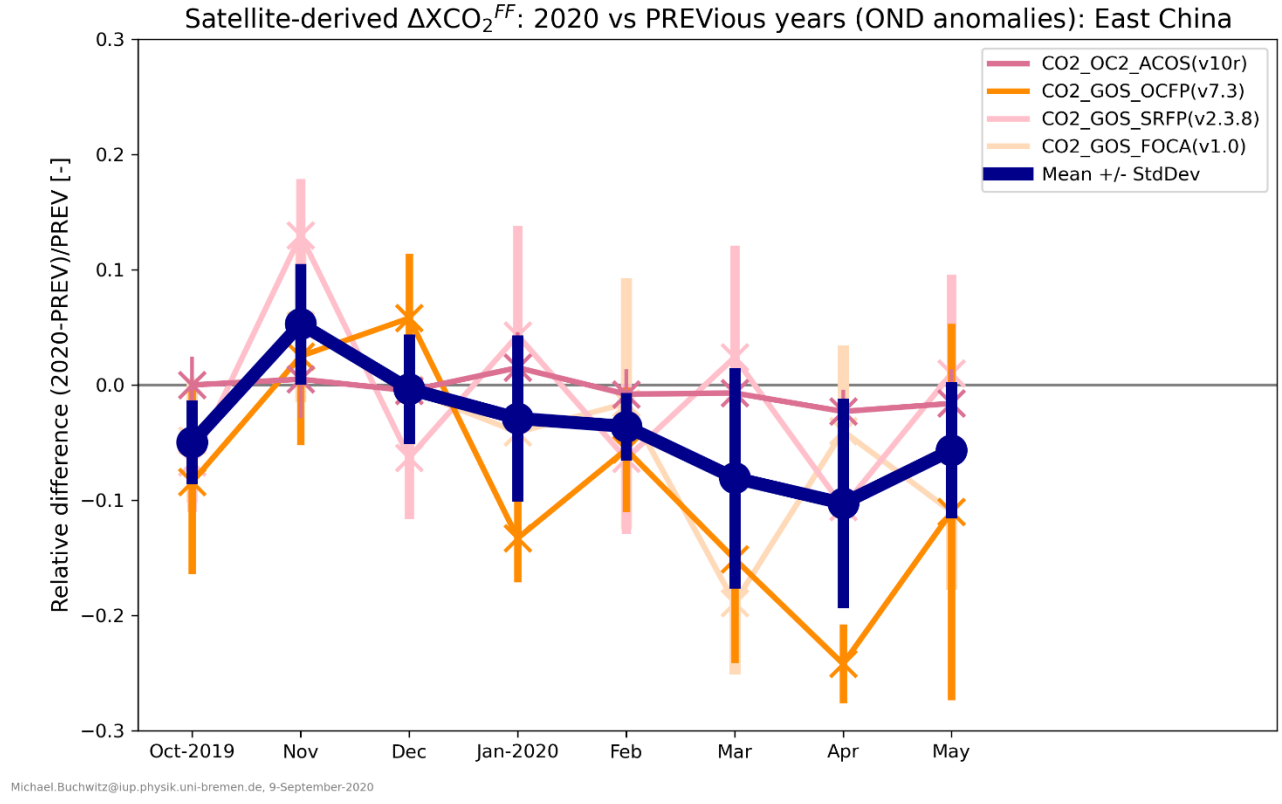

Figure 13: Overview of the ensemble-based ΔXCO_2^{FF} results for January-May 2020 relative to October-December 2019 and previous years (also shown in Figs. 9 – 12) via reddish colours for each of the four analysed satellite XCO_2 data products (see Tab. 1). The corresponding ensemble mean value and its uncertainty is shown in dark blue. The uncertainty has been computed as standard deviation of the ensemble members. The corresponding numerical values of the ensemble members are listed in Tab. 4.